

**Research article**

## Consolidation properties of clay and gyttja soils: A database study

**Monica S Löfman<sup>1,2,\*</sup> and Leena Korkiala-Tanttu<sup>1</sup>**

<sup>1</sup> Department of Civil Engineering, Aalto University, Rakentajanaukio 4, 02150 Espoo, Finland

<sup>2</sup> Ramboll Finland Ltd, Itsehallintokuja 3, 02600 Espoo, Finland

\* Correspondence: Email: monica.lofman@aalto.fi; Tel: +358505111723.

**Abstract:** When constructing on clay and gyttja soils, low-carbon ground improvement methods such as preloading should be preferred over carbon-intensive solutions (e.g., piles or deep mixing with lime-cement binder). The design of preloading requires knowledge about the compressibility and consolidation properties of subsoil, but site-specific oedometer tests may be scarce or even lacking, especially in the early design phases. Hence, this paper presents two extensive databases based on oedometer tests performed on Finnish clay and gyttja soils, with a special emphasis on consolidation rate and creep properties. The FI-CLAY-oedo/14/282 database contains 282 oedometer test-specific data entries, such as initial hydraulic conductivity and maximum creep coefficient. The second database, FI-CLAY-cv/8/774, contains 774 load increment-specific data entries (e.g., coefficient of consolidation) from 232 oedometer tests. The analysis of these databases provided three main results: (i) statistics for bias factors, which quantify the differences between determination methods (log time vs. square root time method and oedometer vs. falling head test), (ii) transformation models (and their transformation uncertainty) to predict creep coefficient from index or consolidation properties, and (iii) typical value distributions for various consolidation rate and creep properties, in a form of histograms and fitted lognormal distributions. All the results are given with statistical information, which allows their straightforward utilization as input data for probabilistic assessment (reliability-based design). It is concluded that the consolidation properties of clay and gyttja soils are indeed characterized by significant uncertainty. Hence, such results are recommended to be used as existing (prior) knowledge when determining design parameters, either by supporting engineering judgement or via a more systematic framework such as Bayesian statistics.

**Keywords:** clay; gyttja; coefficient of consolidation; creep; secondary consolidation; hydraulic conductivity; soil database; model bias; transformation model

---

## 1. Introduction

Construction on soft soils such as clay and gyttja usually requires pile foundations or extensive ground improvement. However, the carbon footprint of such geotechnical solutions is often significant; hence, low-carbon ground improvement methods such as preloading should be preferred over carbon-intensive solutions (e.g., piles or deep mixing with lime-cement binder) [1,2].

The design of preloading (with or without vertical drains) requires knowledge on the geotechnical properties of the soil to be treated; besides compressibility properties such as compression index ( $C_C$ ) and preconsolidation pressure, the time-settlement prediction requires consolidation rate properties such as the coefficient of consolidation ( $c_v$ ) or hydraulic conductivity ( $k$ ) [3,4]. Further, especially in organic soils such as gyttja, the secondary (creep) settlement should also be estimated, e.g., via the creep coefficient ( $C_{ae}$ ). These consolidation rate and creep parameters can be defined using oedometer tests performed on undisturbed samples; the incrementally loaded oedometer test (ILOT) provides all these properties, while the constant rate of strain (CRS) test is usually applied to estimate  $c_v$  and/or  $k$  only (i.e., the standard procedure does not provide estimate for  $C_{ae}$ ). However, acquiring a sufficient amount of high-quality soil samples for the oedometer tests is not realistic in the early stages of the project, and thus, the preliminary settlement analysis is often conducted using literature values and empirical correlations.

In Finland, marine soft clays and gyttja soils are common, especially in the coastal area. Many of these soft soils are sensitive and characterized by very low hydraulic conductivity due to high clay content [5–7]. Some indicative values for the consolidation rate properties of Finnish clays have been presented in design handbooks; however, such table values are scarce and have not been re-evaluated during the last decades. A few Finnish clay databases have been published so far, including FI-CLAY/14/856 [6] and F-CLAY/7/216 [7] in the TC304 compendium of databases (“304dB”), but none of them contain consolidation rate or creep properties. Hence, this paper presents an extensive database of oedometer tests performed on clay and gyttja soils, with a special emphasis on consolidation rate and creep properties. The studied sites are located in Finland, and testing was done at Aalto University (previously the Technical University of Helsinki) for various research projects. Two databases were compiled. The first, FI-CLAY-oedo/14/282, contains 282 oedometer test results, some of which are enhanced with classification test results from a nearby specimen (i.e., partially multivariate database). The 14 parameters of interest in FI-CLAY-oedo/14/282 are the maximum creep coefficient ( $C_{ae,max}$ ), initial hydraulic conductivity from ILOT ( $k_I$ ), minimum coefficient of consolidation from CRS ( $c_{v,min}$ ), natural water content ( $w_n$ ), initial void ratio ( $e_0$ ), fall cone liquid limit ( $F$ ), undrained shear strength ( $s_u$ ), sensitivity ( $S_I$ ), degree of saturation ( $S_r$ ), effective in situ stress ( $\sigma_{v0}'$ ), preconsolidation pressure ( $\sigma_p'$ ), over-consolidation ratio (OCR), compression index ( $C_C$ ), and swelling index ( $C_s$ ). The second database is named FI-CLAY-cv/8/774 and contains 774 load increment-specific data entries from 232 ILOT tests. The eight parameters of interest in FI-CLAY-cv/8/774 are the square root time (Taylor) coefficient of consolidation ( $c_{vT}$ ), log time (Casagrande) coefficient of consolidation ( $c_{vC}$ ), creep coefficient ( $C_{ae}$ ), Taylor hydraulic conductivity ( $k_T$ ), Casagrande hydraulic conductivity  $k_C$ , falling head test hydraulic conductivity ( $k_{direct}$ ), stress ratio ( $\sigma_v'/\sigma_p'$ ), and  $w_n$ . Many of the oedometer tests included in the newly compiled FI-CLAY-oedo/14/282 are also included in the previously published FI-CLAY/14/856 [6]; the key difference between the databases is that FI-CLAY/14/856 did not contain any consolidation rate properties (e.g.,  $k_I$  or  $C_{ae,max}$ ) nor stress increment data. Indeed, Löfman and Korkiala-Tanttu [6] used the previously published database to derive transformation models for

compression indices  $C_C$  and  $C_S$ , while this paper investigates the consolidation rate ( $k$ ,  $c_v$ ) and creep properties ( $C_{ae}$ ).

These newly compiled databases are used to characterize the consolidation rate and creep properties of soft marine clays and gyttjas by means of statistics and histograms (typical value distributions). The systematic differences between methods (e.g., log time vs. square root time method) to define consolidation properties are defined via bias factors. In addition, transformation models to predict consolidation properties based on other geotechnical properties (e.g.,  $w_n$ ) are investigated and derived. It should be noted that although the compiled database FI-CLAY-oedo/14/282 also includes compressibility properties (e.g.,  $C_C$ ), this study focuses on consolidation rate and creep properties only. The derived typical value distributions and transformation models can be used as input parameters for the preliminary settlement predictions done in the early stages of preloading design, when no site-specific oedometer tests are available. The results may also be applied to evaluate the reliability of oedometer tests and as existing knowledge to consider when determining the characteristic value. Bayesian statistics, for example, allow a systematic framework to combine existing knowledge (e.g., typical value distributions) with limited site-specific ground investigations as prior distributions [8–10].

## 2. Materials and methods

### 2.1. Characterization of consolidation properties

Consolidation properties (coefficient of consolidation  $c_v$ , hydraulic permeability  $k$ , and creep coefficient  $C_{ae}$ ) can be defined with an ILOT test. For each load increment, a time-settlement graph is constructed to define  $c_v$  and  $C_{ae}$ . Figure 1a presents the principle of determining  $c_v$  using the square root time method, also known as the Taylor method [11]. This method is based on finding the time and specimen height corresponding to a 90% degree of primary consolidation ( $U$ ). The coefficient of consolidation  $c_{vT}$  is calculated as follows:

$$c_{vT} = \frac{0.848H^2}{t_{90}} \quad (1)$$

where drainage length  $H$  is equal to half of the specimen thickness at  $U = 50\%$  consolidation, and  $t_{90}$  is the time at  $U = 90\%$  (0.484 is the time factor corresponding to  $U = 90\%$ ).

The log time method, also known as the Casagrande method [12], is illustrated in Figure 2a; a 100% degree of primary consolidation is interpreted using the extrapolated line fitted to the steepest tangent and the line fitted to the secondary (creep) settlement observations. The coefficient of consolidation  $c_{vC}$  is then calculated with the time and specimen height corresponding to  $U = 50\%$ :

$$c_{vC} = \frac{0.196H^2}{t_{50}} \quad (2)$$

As illustrated in Figure 1b, the creep coefficient  $C_{ae}$  is acquired as the slope of creep settlement line [13]:

$$C_{ae} = \frac{\Delta \varepsilon_s}{\Delta \log(t)} \quad (3)$$

where  $\varepsilon_s$  is compression during secondary consolidation (%). The unit for  $C_{ae}$  is usually %. An alternative formulation is based on void ratio ( $e$ ) change instead of compression (creep coefficient  $C_{ae}$ ).

Usually, the interpretation of  $C_{ae}$  requires rather long consolidation times for the creep to occur; for Finnish soft soils, the standard time of 24 h usually provides reasonable estimates. However, more complete characterization of creep behavior requires longer ( $>24$  h) load increments (this test type is later referred to as *ILOT\_CREEP*).

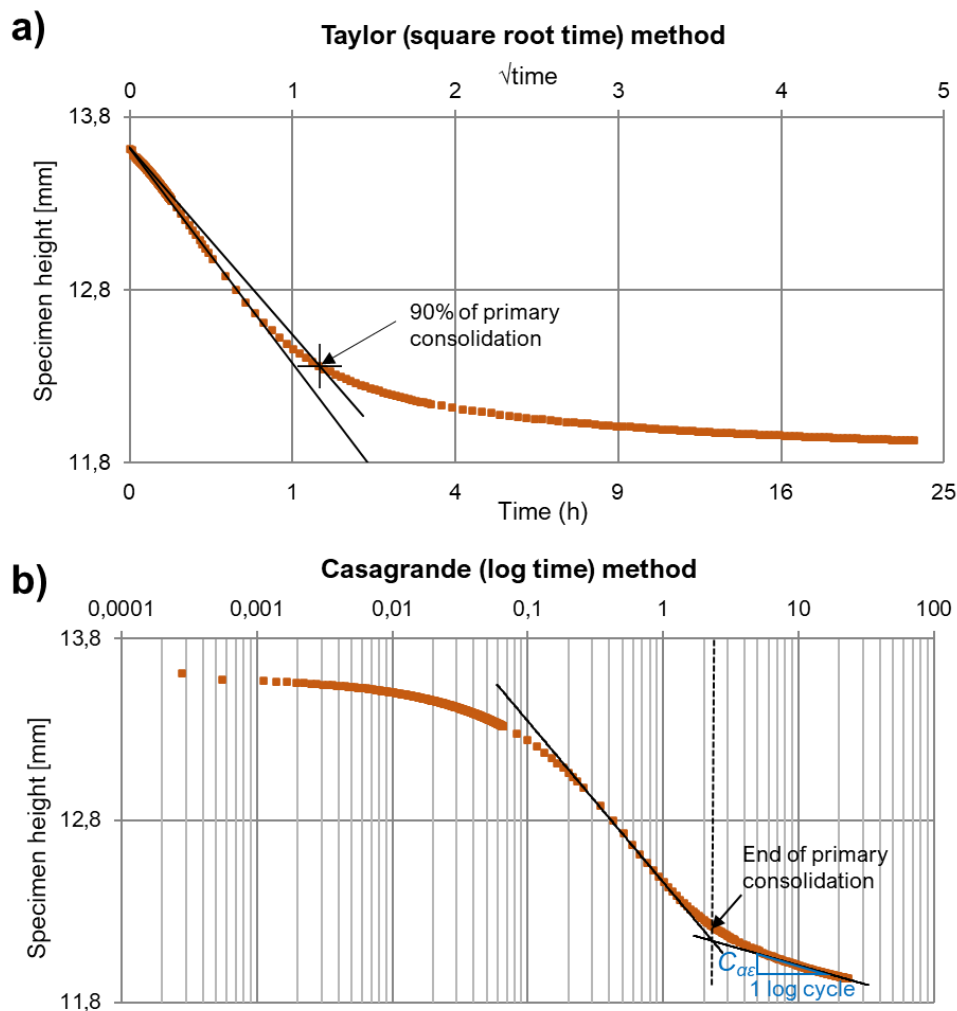


**Figure 1.** Determination of consolidation properties ( $c_v$  and  $C_{ae}$ ) from incremental oedometer test: (a) Taylor method; (b) Casagrande method.

For each load increment, the hydraulic conductivity  $k$  may be estimated using the  $c_v$  value, unit weight of water ( $\gamma_w$ ), and modulus, while assuming that Terzaghi's theory of consolidation is valid:

$$k = \frac{c_v \gamma_w}{M_s} \quad (4)$$

where oedometer modulus  $M_s$  is defined for the load increment in question via  $\Delta\sigma_v'/\Delta\varepsilon_v$ , where  $\varepsilon_v$  is vertical compression, and  $\sigma_v'$  is effective vertical stress.

Typically, the parameter of interest is the vertical coefficient of consolidation  $c_v$ , to be used as input for one-dimensional settlement calculation. However, if preloading with vertical drains is used,

the horizontal consolidation properties may be investigated using rotated soil samples or a special radial consolidation oedometer test (later referred to as *ILOT\_H*).

Once the stress increments have been analyzed, the oedometer curve may be constructed using the interpreted end-of-primary (EOP) [14] compression points (see Figure 2). Preconsolidation pressure  $\sigma'_p$  separates the over-consolidated (OC) stress state and normally-consolidated (NC) stress state for the soil specimen. As illustrated in Figure 2, the  $c_v$  values are typically quite high in the OC region and tend to drop significantly after  $\sigma'_p$ . After the minimum  $c_v$ , a moderate increase is often observed with increasing stress. Figure 2 also shows the applied interpretation method for compression index  $C_C$ , which emphasizes the compressibility right after  $\sigma'_p$  rather than the whole NC curve, since the soft sensitive clays in Finland typically exhibit nonlinear behavior also in a semi-logarithmic space.

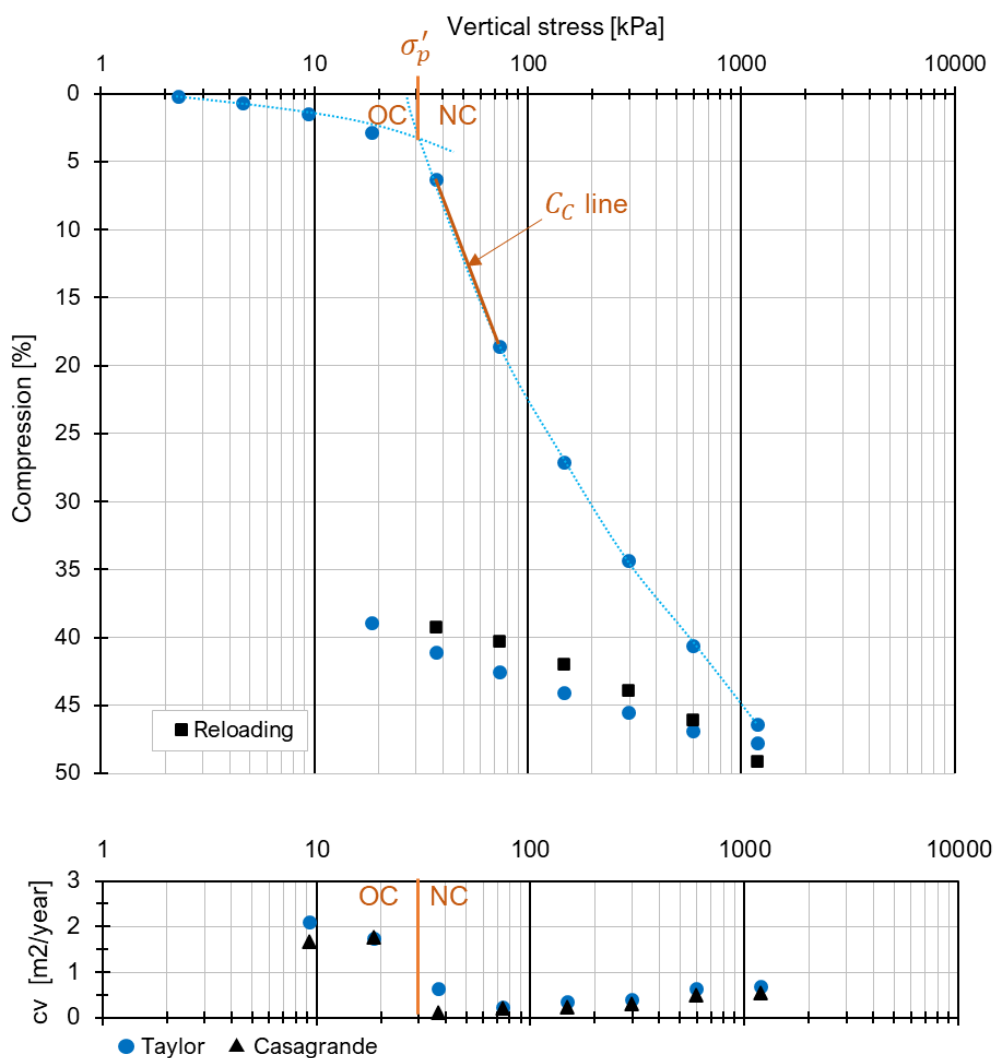


**Figure 2.** Example of a stress-strain relationship for a clay specimen and changes in the coefficient of consolidation,  $c_v$ , with stress.

Hydraulic conductivity  $k$  exhibits some decrease with increasing compression, as the pore space is increasingly reduced (see Figure 3). The initial hydraulic conductivity at the beginning of the oedometer test ( $k_i$ ) may be interpreted by a linear regression fitted to the logarithm of  $k$ :  $k$  at zero

compression is then found by extrapolation [15]. When fitting the regression line,  $k$  values corresponding to the first few load increments (in the OC region) may be omitted if needed, since the time-settlement analyses are not as accurate in the OC stress state as they are in NC stress state with classical time-settlement behavior. In addition, there may be some unevenness in the oedometer test specimen's surface at the beginning of the test, which leads to inaccuracies. Quite often, the OC state time-settlement analysis is not performed at all, and the first  $k$  value corresponds to compression around 5–20%; In such a case, using that  $k$  value as initial  $k$  would be an underestimation.

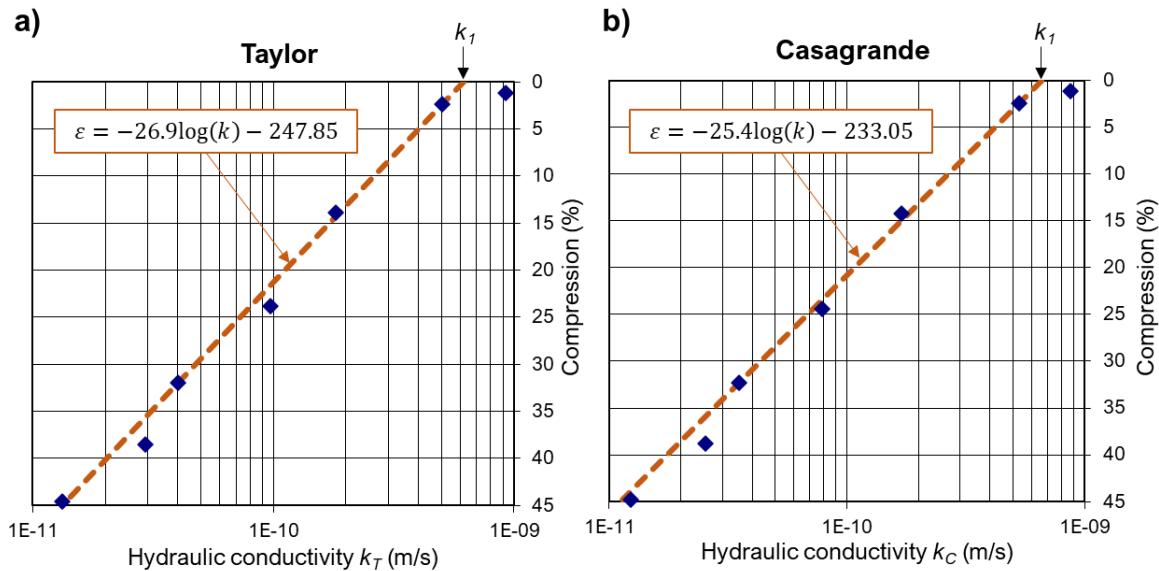


**Figure 3.** Example of a hydraulic conductivity  $k$  reducing with compression and the interpretation of initial  $k_1$  from  $k$  values based on (a) Taylor method and (b) Casagrande method.

The creep coefficient  $C_{ae}$  also exhibits stress dependency:  $C_{ae}$  is very low until a certain stress and compression are reached, after which it increases fast up to a maximum value and then slowly decreases with further compression (see an example in Figure 4). Indeed, Mesri et al. [16] suggested that the ratio  $C_{ae}/C_C$  is constant, thus implying that maximum  $C_{ae}$  occurs during maximum compressibility, i.e., right after  $\sigma_p'$  (see Figure 2). On the other hand, subsequent studies have shown that this ratio is not constant in soft sensitive clays (see, e.g., [17]).

In Nordic soft soils, the significant increase in  $C_{ae}$  has been found to occur when vertical effective stress is approximately  $0.8\sigma_p'$  [15]. However, the determination of  $C_{ae}$  with the Casagrande method tends to be unsuccessful in stress regions close to  $\sigma_p'$  due to the time-settlement graph exhibiting a form other than reverse s-shaped. Thus, the maximum  $C_{ae}$  needs to be estimated indirectly. Figure 4b shows the Swedish method [15] based on compression: the linear line is fitted to the observations after the critical compression at  $0.8\sigma_p'$ , and the extrapolated value at critical compression is the estimated  $C_{ae,max}$ . Alternatively,  $C_{ae,max}$  is interpreted using the stress method, i.e., via the  $C_{ae}$  values at stresses greater than  $0.8\sigma_p'$  or  $\sigma_p'$  (see, e.g. [18]). In the stress method (see Figure 4a), the decrease in  $C_{ae}$  after the maximum tends to be less linear, and hence the interpretation may vary; wider coverage of stresses often provides a less conservative estimate for  $C_{ae,max}$ , compared to focusing on the stresses right after  $0.8\sigma_p'$ .

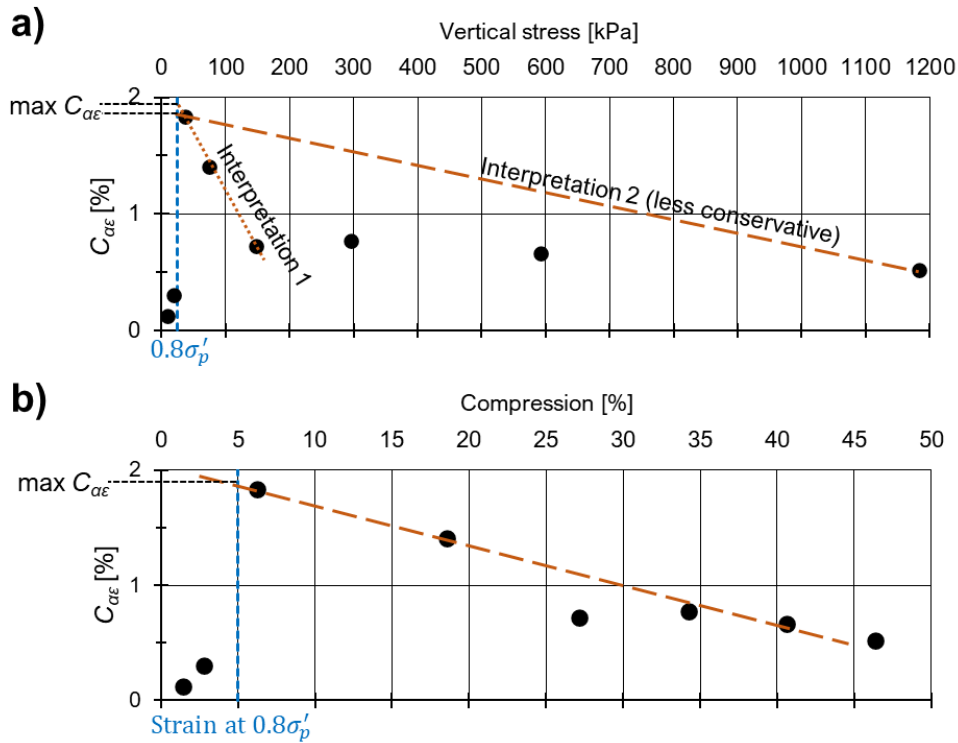


**Figure 4.** Estimation of maximum creep coefficient  $C_{ae,max}$  using the (a) stress method (e.g., [18]) and (b) compression method [15].

## 2.2. Databases FI-CLAY-oedo/14/282 and FI-CLAY-cv/8/774

The compiled oedometer test database FI-CLAY-oedo/14/282 is partially multivariate. The included parameters and their statistics are collected in Table 1. Each row in this database represents one oedometer test. In the database name, 14 refers to the number of main parameters of interest; it should be noted, however, that the database contains more than 14 columns, providing some additional information. The number 282 refers to the number of data rows (i.e., oedometer tests). Table 1 summarizes the statistics for the soil parameters included in the database. All the data rows include natural water content  $w_n$ , initial void ratio  $e_0$ , (bulk) unit weight  $\gamma$ , and initial hydraulic conductivity  $k_l$ . On the other hand, there are only 168 oedometer tests with  $C_{ae,max}$ . Statistics of the degree of saturation show that the specimens were fully saturated, with a few exceptions with  $S_r < 100\%$ .

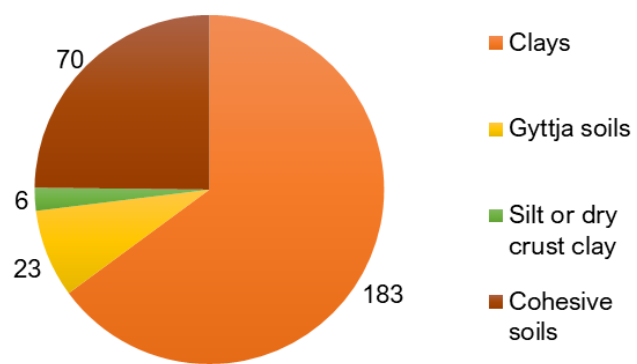
From the 282 oedometer tests, 65% are ILOT tests, while the rest are CRS tests. Some of the ILOT tests ( $n = 25$ ) were combined with the falling head test (test type “ILOT\_K”), which allows direct measurement of hydraulic conductivity ( $k_{direct}$ ). The database contains  $n = 12$  long-term oedometer tests (“ILOT\_CREEP”) and  $n = 19$  horizontal oedometer tests (“ILOT\_H”). As the portion of these special tests is relatively small, these test results have not been filtered out in the analysis.

The clear majority of test specimens in FI-CLAY-oedo/14/282 are clays (see Figure 5). About 25% of specimens are estimated to be clays, gyttja soils, or silts, thus classified as cohesive soils (since actual classification data was lacking). The applied “GEO” soil type classification system is based on geological origin, grain size distribution, and organic content [19].

**Table 1.** Statistics for the oedometer test database FI-CLAY-oedo/14/282.

Property	Unit	Symbol	n	Mean	SD <sup>a)</sup>	Min	25%	50%	75%	Max
Natural water content	%	$w_n$	282	94.37	34.92	28.00	69.92	92.15	110.00	187.00
Void ratio	—	$e_0$	282	2.56	0.93	0.78	1.89	2.52	3.02	5.20
Unit weight	kN/m <sup>3</sup>	$\Gamma$	282	14.94	1.56	11.95	13.98	14.74	15.80	19.61
Hydraulic conductivity, ILOT <sup>c)</sup>	$10^{-9}$ m/s	$k_l$	282	1.37	2.23	0.07	0.53	0.86	1.43	30.20
Max. creep coefficient, stress method	%	$C_{ac,max}$	168	1.90	1.36	0.13	0.92	1.48	2.66	7.73
Degree of saturation	%	$S_r$	224	99.02	3.27	66.00	99.00	100.00	100.00	107.46
Effective in situ stress	kPa	$\sigma_{v0}'$	241	38.70	24.97	3.00	20.24	32.00	48.50	143.00
Preconsolidation stress	kPa	$\sigma_p'$	262	62.69	53.37	10.00	30.00	43.00	74.75	350.00
OCR	—	OCR	227	1.69	1.21	0.42	1.03	1.33	1.77	10.58
Compression index	—	$C_c$	240	1.53	0.87	0.07	0.80	1.45	2.09	4.64
Swelling index	—	$C_s$	227	0.11	0.09	0.01	0.06	0.10	0.14	0.94
Min. coefficient of consolidation, CRS test	m <sup>2</sup> /year	$c_{v,min}$	94	0.81	2.23	0.05	0.19	0.26	0.56	19.60
Fineness number <sup>b)</sup>	(%)	$F$	76	80.10	37.78	38.67	57.08	69.70	85.57	202.30
Undrained shear strength	kPa	$s_u$	81	34.46	27.95	10.50	18.40	25.80	37.30	156.90
Sensitivity	—	$S_t$	76	18.68	11.47	1.40	9.75	16.94	24.70	46.97
Organic content	%	Org	68	1.33	2.18	0.00	0.00	0.21	1.85	9.20
Clay content	%	Cl	62	54.42	18.18	23.50	38.38	50.00	68.25	89.00

Note: <sup>a)</sup> SD = sample standard deviation. <sup>b)</sup>  $F$  is the fall cone liquid limit, which has been found to be approximately equal to liquid limit  $w_L$  [6]. <sup>c)</sup> The majority of  $k_l$  values were interpreted using the Taylor method (see Figure 3a).

**Figure 5.** Soil types included in the FI-CLAY-oedo/14/282 database.

The second compiled database, FI-CLAY-cv/8/774, contains stress increment-specific information from ILOT tests. That is, each row represents the interpreted parameters from one load increment. Test-specific properties such as test number, water content of the specimen, and preconsolidation pressure are thus repeated for each load increment. Table 2 represents the statistics of

the included parameters. This database contains results from 232 ILOT tests, some of which have been performed on rotated specimens to study horizontal permeability ( $n = 41$  data rows out of  $n = 774$  load increments). In total, 138 ILOT tests in FI-CLAY-cv/8/774 are also included in the FI-CLAY-oedo/14/282 database. Most of the specimens included in the FI-CLAY-cv/8/774 database were estimated to represent clay or gytta soils.

**Table 2.** Statistics for the load increment database FI-CLAY-cv/8/774.

Property	Unit	Symbol	n	Mean	SD	Min	25%	50%	75%	Max
Effective vertical stress (in the beginning of load increment)	kPa	$\sigma_v'$	774	199.62	240.66	7.35	50.00	100.00	201.00	1487.00
Coefficient of consolidation, square root time (Taylor)	$\text{m}^2/\text{year}$	$c_{vT}$	774	6.58	14.17	0.02	0.28	0.80	4.42	93.85
Coefficient of consolidation, log time (Casagrande)	$\text{m}^2/\text{year}$	$c_{vC}$	704	3.81	9.17	0.01	0.18	0.47	2.07	79.44
Creep coefficient	%	$C_{ae}$	699	1.05	0.92	0.02	0.40	0.79	1.47	6.40
Hydraulic conductivity, square root time (Taylor)	$10^{-9} \text{ m/s}$	$k_T$	398	0.47	0.56	0.00	0.11	0.28	0.62	4.39
Hydraulic conductivity, log time (Casagrande)	$10^{-9} \text{ m/s}$	$k_C$	382	0.32	0.39	0.00	0.08	0.19	0.41	2.77
Hydraulic conductivity, falling head test	$10^{-9} \text{ m/s}$	$k_{direct}$	49	0.40	0.28	0.09	0.18	0.30	0.57	1.36
Preconsolidation stress	kPa	$\sigma_p'$	772	79.46	76.03	7.00	27.00	46.00	97.89	350.00
Stress ratio	–	$\sigma_v'/\sigma_p'$	770	3.72	5.06	0.04	1.09	2.17	4.30	61.54
Natural water content	%	$w_n$	774	87.38	35.73	18.60	58.34	84.40	113.00	178.20
Degree of saturation	%	$S_r$	488	99.44	2.71	84.00	99.25	100.00	100.00	107.46
Effective in situ stress	kPa	$\sigma_{v0}'$	764	40.86	28.25	4.00	20.00	31.50	53.00	143.00
OCR	–	OCR	762	2.14	2.25	0.10	1.00	1.42	2.26	27.00

Table 3 presents the included sites, sampling years, and number of observations in both databases. All the sites are located in Finland; the majority are located on the southern or western coast of Finland. More detailed references for the test data are given in the database info (see supplementary material). Most of the included study sites are described in greater detail by Löfman and Korkiala-Tanttu [6], as they are also included in the previously published database FI-CLAY/14/856.

### 2.3. Transformation uncertainty and model bias

Empirical correlations (transformation models) are characterized by transformation uncertainty [21]; that is, the model to predict a consolidation property using another soil parameter is never perfect. Bias factor is a useful variable for evaluating the systematic and random transformation uncertainty. The bias factor  $b_i$  of  $i$ th data point can be defined as the actual target value (e.g.,  $C_{ae}$ ) divided by the predicted target value (e.g., prediction based on  $w_n$ ) [22]:

$$b_i = \frac{\text{actual target value}}{\text{predicted target value}} \quad (5)$$

The model bias  $b$  is the arithmetic mean of values  $b_i$ . If  $b = 1$ , the model is unbiased (i.e., no systematic transformation error). The (random) transformation uncertainty can be defined from the sample coefficient of variation (COV) of values  $b_i$ , usually denoted by  $\delta$ . Sample COV is a measure of data dispersion, which is defined as the sample SD divided by the mean, and it is sometimes given as a percentage. The definition of transformation uncertainty via  $\delta$  represents a multiplicative form [22]:

$$\text{actual target value} = \text{predicted target value} \times b \times \varepsilon_{\text{trans}} \quad (6)$$

where  $\varepsilon_{\text{trans}}$  is the variability term (random variable) for the transformation model. The mean of  $\varepsilon_{\text{trans}}$  is 1, and its COV is  $\delta$ .

In addition to the evaluation of transformation models, the bias factor may be applied to study the systematic difference between various methods to define consolidation properties (e.g.,  $k$  from oedometer or direct measurement,  $c_v$  based on Taylor's or Casagrande's method). For example, if the bias factor is defined as  $k_{\text{direct}}/k_T$ , model bias  $b > 1$  means that the falling head test, on average, provides greater  $k$  values than the Taylor method.

**Table 3.** Description of the included sites (FI-CLAY-oedo/14/282 and FI-CLAY-cv/8/774).

Site	Reference	Sampling year(s)	FI-CLAY-oedo/14/282 $n (k_I)$	FI-CLAY-cv/8/774 $n (c_{vT})$
Haarajoki	[6]	1995	23	22
Ossinlampi, Otaniemi (HUT-clay)	[6]	2009, 2012	17	27
Kimola (canal)	[6]	2017	20	123
Kujala test embankments (Lahti vt12)	[6]	2017	26	106
Murro (test embankment)	[6]	1993	1	2
Maarinranta, Otaniemi	[6]	1998	(0)	68
POKO (Porvoo-Koskenkylä)	[6]	1999	55	81
Perniö (test embankment)	[6]	2009, 2010	11	47
Suurpelto (Espoo)	[6]	2005, 2008	31	94
Söderkulla-Nikkilä (Sipoo, Pt 11689)	[6]	1997–1999	47	86
Tattara (Nakkila, Pt 12895)	[6]	1997	(0)	18
Tolsa (Kirkkonummi)	[6]	1996	(0)	7
Vanttila (Espoo)	[20]	2001/2002 <sup>b)</sup>	10	33
Östersundom (test embankment)	[6]	2013	41	(0)

Note: <sup>b)</sup> Estimated.

#### 2.4. Linear and polynomial regression models (transformation models)

This section describes the methodology to derive transformation models for consolidation properties. To be more specific, this paper applies linear and polynomial regression models fitted using

the ordinary least squares (OLS) method within the Scikit-learn library for Python [23]. The polynomial transformation model and its transformation uncertainty are defined by:

$$\hat{Y} = b_0 + b_1 X + b_2(X)^2 + \varepsilon \quad (7)$$

where  $\hat{Y}$  is the predicted ln-transformed target value,  $b$  terms are regression coefficients,  $X$  is the ln-transformed predictor, and  $\varepsilon$  is the transformation error. Error  $\varepsilon$  is a zero-mean normal random variable with standard deviation  $\sigma_\varepsilon$  (additive transformation uncertainty). OLS is applied to natural logarithms of the soil properties to ensure relatively constant residual scatter around the trendline. The linear regression model is otherwise similar to Equation 7, but the coefficient  $b_2$  is zero.

Transformation error  $\varepsilon_i$  for  $i$ th data point is quantified as the residual (error) term of  $i$ th observation (e.g.,  $C_{ae,max}$  from ILOT test) minus the predicted value  $\hat{Y}$ . The standard deviation of the transformation error  $\sigma_\varepsilon$  can then be estimated from these individual residual errors using Equation 8 (see, e.g., [24]):

$$\sigma_\varepsilon = \sqrt{\frac{1}{n-v} \sum_{i=1}^n [Y_i - \hat{Y}_i]^2} \quad (8)$$

where  $n$  is the number of observations used in the linear regression, and  $v$  is the number of degrees of freedom (here taken as the number of estimated regression coefficients).

Before fitting the transformation model, potential outliers need to be detected and removed. In this study, creep coefficients ( $C_{ae,max}$  or  $C_{ae}$ ) greater than 6 were not considered, as they were observed to be very rare;  $n = 2$   $C_{ae,max}$  values and one  $C_{ae}$  were thus removed as outliers. In addition, for each transformation model, the standard deviation method with a  $3\sigma$ -threshold was applied; those data points in which the residual error  $\varepsilon_i$  was more than  $3\sigma_\varepsilon$  apart from the zero mean were detected as outliers and thus removed before defining the final regression coefficients and model statistics.

### 3. Results and discussion

#### 3.1. Stress dependency of consolidation properties

As illustrated in Figure 6, the stress dependency of the coefficient of consolidation  $c_v$  is clearly visible in the compiled database FI-CLAY-cv/8/774. In NC state,  $c_v$  tends to be less than  $2 \text{ m}^2/\text{year}$  for the considered marine soft soils. Similarly, the creep coefficient  $C_{ae}$  shows a clear distinction between the critical stress ratio  $\sigma_v'/\sigma_p' = 0.8$  (see Figure 7). The figure also shows that variability in  $C_{ae}$  is smaller in the OC stress state (stress ratio  $< 0.8$ ) than in the NC stress state, where higher  $C_{ae}$  values are observed. In preloading design,  $C_{ae}$  in the OC state may be used to estimate creep settlement after the removal of temporary surcharge, since the subsoil behaves as over-consolidated soils if the preloading has been successful.

#### 3.2. Model biases: Coefficient of consolidation and hydraulic conductivity (FI-CLAY-cv/8/774)

This analysis uses the bias factors to compare different methods used to define  $c_v$  or  $k$ . Figures 8 and 9 compare the Taylor and Casagrande methods to define  $c_v$  or  $k$ , respectively. Figures 8b and 9b show the histograms of bias factors ( $c_{vC}/c_{vT}$  or  $k_C/k_T$ ) and the fitted distribution(s). Normal distribution was fitted to the data using the method of moments (MoM), while a lognormal distribution was fitted

using the maximum likelihood estimation method (MLE). The results of the bias analysis are shown in Table 4. The arithmetic mean for the bias factor  $c_{vC}/c_{vT}$  is  $b = 0.8$ , meaning that the coefficient of consolidation  $c_v$  defined using the Casagrande method is, on average,  $0.8c_{vT}$ . In other words,  $c_v$  defined using the Taylor method tends to be higher, on average  $1.25c_{vC}$  ( $1/0.8 = 1.25$ ). The bias factor  $k_C/k_T$  has quite very similar statistics, but the histogram shows a different shape: the lognormal distribution did not provide a good fit and was hence omitted from the results (see Figure 9b). The authors estimate that the main reason for the model bias is that while the Taylor method emphasizes the initial part of the time-settlement curve, the Casagrande method utilizes measurements all the way until  $U \approx 100\%$ , where creep also starts to influence the time-settlement behavior besides primary consolidation.

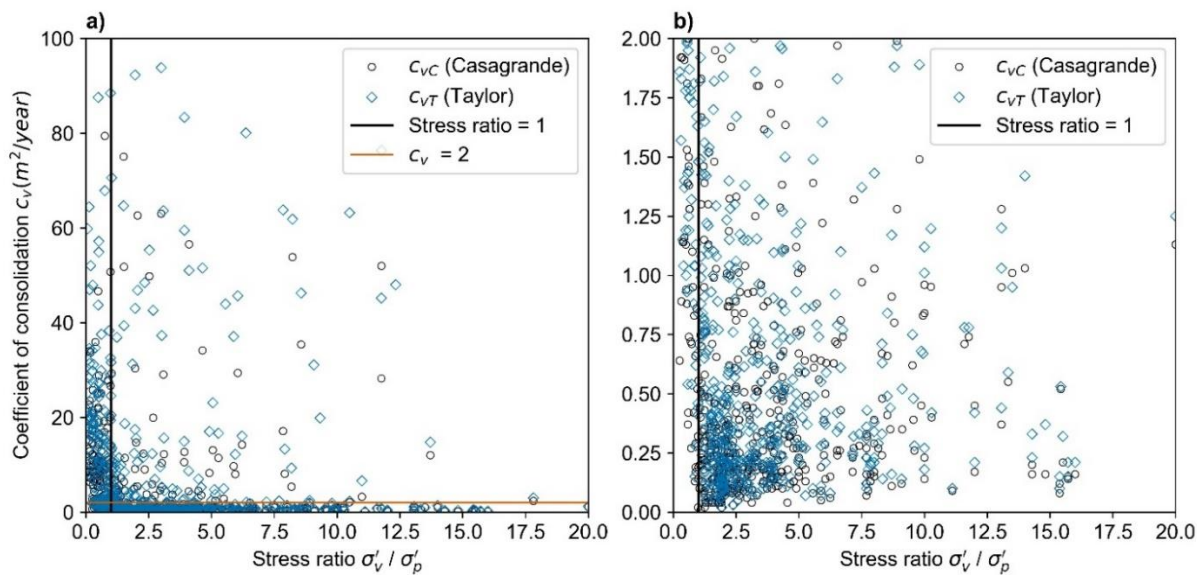


**Figure 6.** Coefficient of consolidation  $c_v$  as a function of stress ratio: (a) all observations; (b)  $c_v = 0\text{--}2 \text{ m}^2/\text{year}$  (FI-CLAY-cv/8/774).

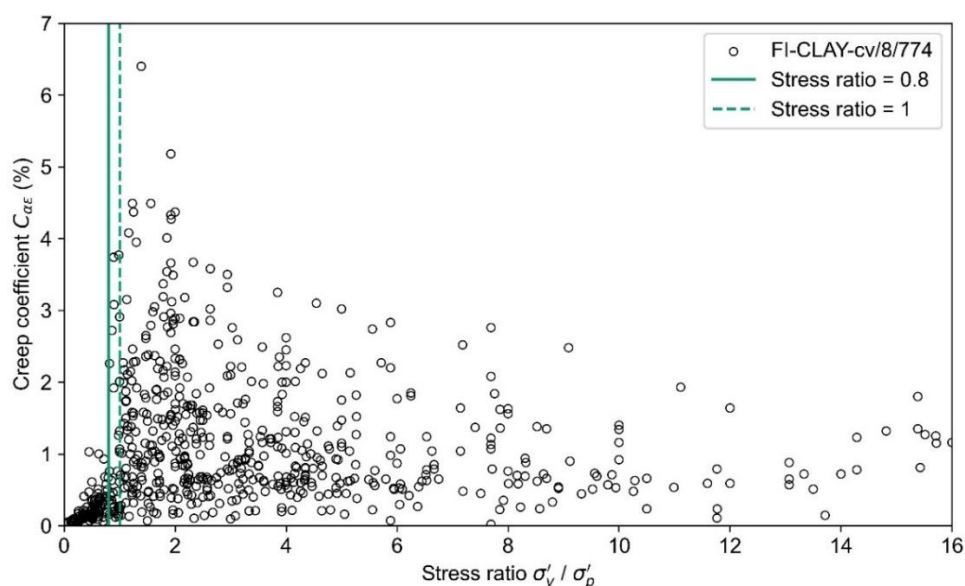


**Figure 7.** Creep coefficient  $C_{\alpha c}$  as a function of stress ratio (FI-CLAY-cv/8/774).

Figure 10 describes the model bias for estimating  $k$  from the ILOT test ( $k_C$  or  $k_T$ ) compared with the falling head test ( $k_{direct}$ ). According to Figure 10, a lognormal distribution provides a better fit compared to a normal distribution. The mean bias factors for the Taylor and Casagrande methods are 1.67 and 2.35, respectively; that is,  $k_T$  is less biased on average. In addition, the COV value for the bias factor is smaller for  $k_T$  (0.52 compared to 0.92), which indicates smaller model uncertainty. However, the studied sample size was rather small ( $n = 47$ –49 bias factors).

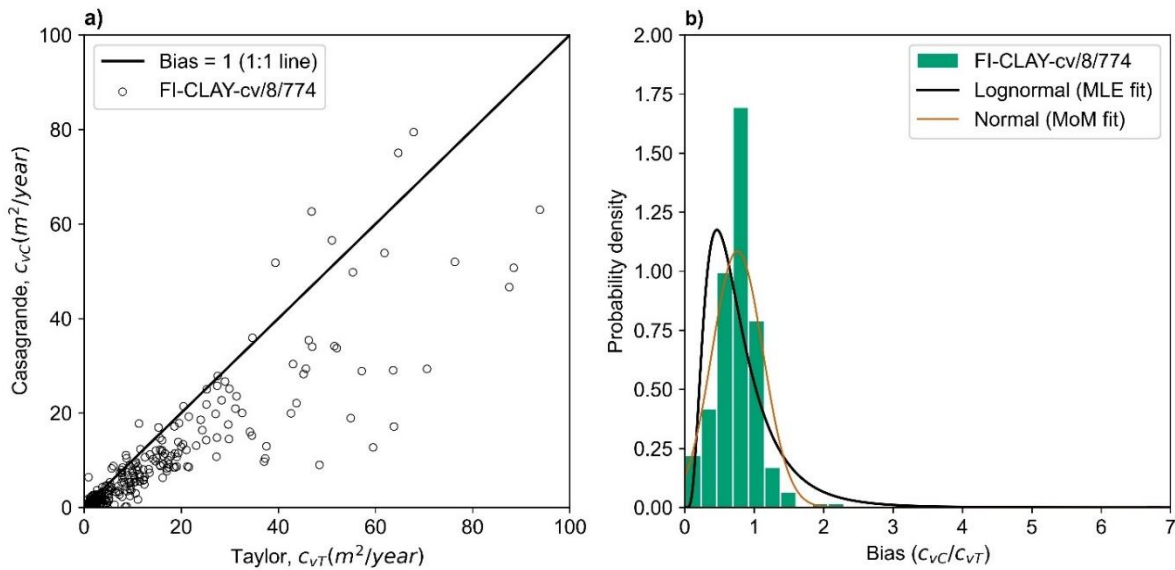


**Figure 8.** Bias between Taylor (root time) and Casagrande (log-time) methods: (a) coefficient of consolidation  $c_{vT}$  vs.  $c_{vC}$ ; and (b) histogram and fitted distributions for bias  $c_{vC}/c_{vT}$ .

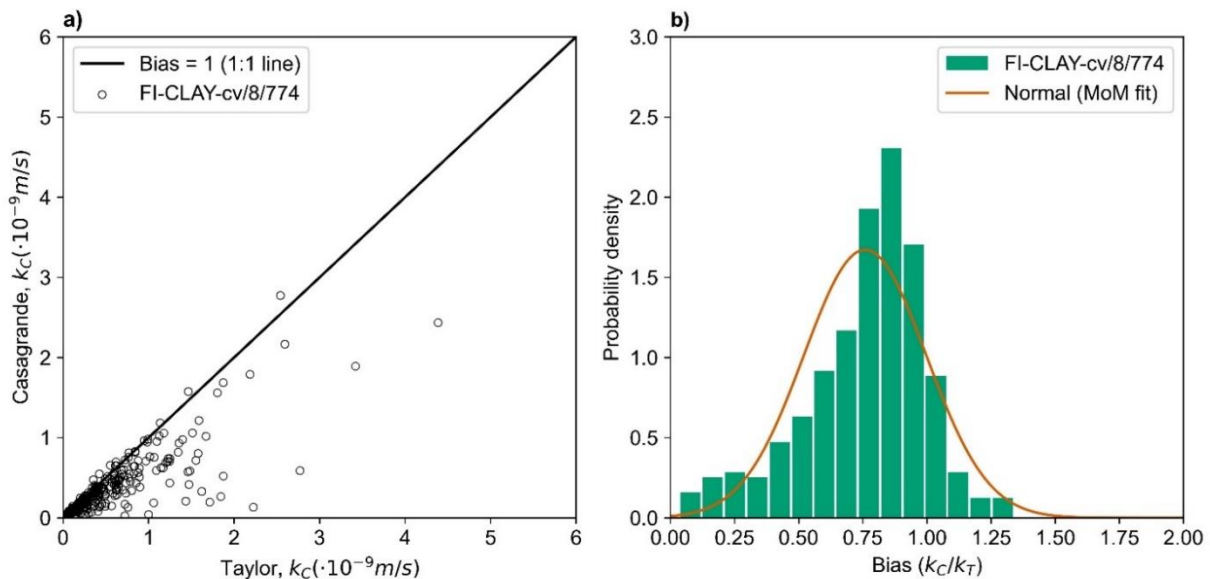


**Figure 9.** Bias between Taylor (root time) and Casagrande (log-time) methods: (a) hydraulic conductivity  $k_T$  vs.  $k_C$ ; (b) histogram and fitted distribution for bias  $k_C/k_T$ .

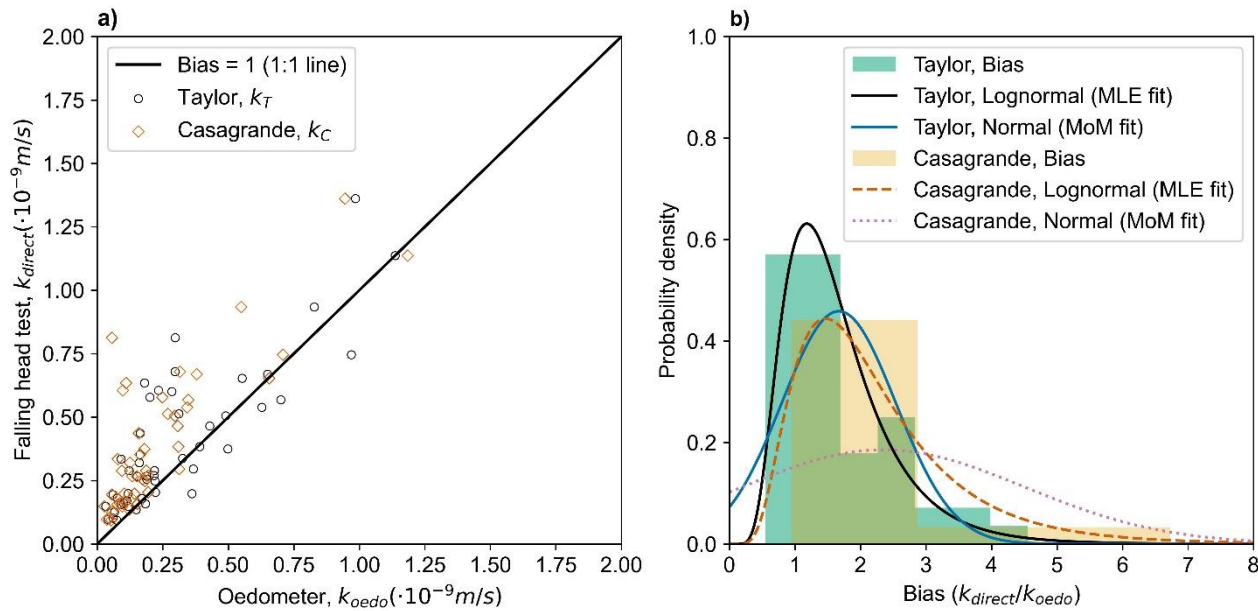


**Figure 10.** Bias between the incremental oedometer and falling head test methods: (a) hydraulic conductivity  $k_{direct}$  vs.  $k_{oedo}$ ; (b) histogram and fitted distributions for bias  $k_{direct}/k_{oedo}$ .

**Table 4.** Statistics for the bias factors and the parameters of the fitted lognormal distribution.

Bias factor	Statistics (arithmetic)							Lognormal distribution	
	$n$	min	50%	max	mean ( $b$ )	SD	COV	$\mu_{ln}$	$\sigma_{ln}$
$c_{vC}/c_{vT}$	704	0.003	0.769	6.88	0.759	0.368	0.484	-0.3998	0.6096
$k_C/k_T$	364	0.035	0.804	1.34	0.759	0.239	0.314	N/A	N/A
$k_{direct}/k_C$	47	0.944	1.761	14.4	2.350	2.150	0.915	0.6662	0.5315
$k_{direct}/k_T$	49	0.547	1.381	4.55	1.669	0.870	0.521	0.3949	0.4771

Notes:  $n$  = number of observations (bias factors); 50% = median;  $b$  = model bias; SD = standard deviation; COV = coefficient of variation;  $\mu_{ln}$  = mean (parameter for lognormal distribution);  $\sigma_{ln}$  = standard deviation (parameter for lognormal distribution).

### 3.3. Transformation models for consolidation properties

#### 3.3.1. Coefficient of consolidation and hydraulic conductivity

This section investigates empirical correlations for consolidation properties that may be used to derive transformation models. Figure 11 shows that  $c_v$  shows some correlation with  $w_n$ : high  $c_v$  values seem to be more common for soils with smaller  $w_n$ , while soft soils with  $w_n > 70\%$  (Figure 11b) are characterized by smaller  $c_v$  values (mostly  $c_v < 2 \text{ m}^2/\text{year}$ ). After ln-transformation, a regression function could be fitted to the data, but the transformation uncertainty was estimated to be too large ( $\delta > 1$ ) for practical use. Instead, typical value distributions were defined for soft soils and stiffer soils separately (see Section 3.4).

Some previous studies (e.g., [25]) found a correlation between  $c_v$  and plasticity index. However, this transformation model could not be investigated because the compiled databases do not include a sufficient number of plasticity index values (as the Finnish geotechnical classification system [19] does not incorporate plasticity index).

Hydraulic conductivity  $k$  has been demonstrated to be correlated with initial void ratio, liquid limit  $w_L$ , and ratio  $w_n/w_L$  ([26]). Figure 12a shows the relationship between  $w_L$  and  $k_L$  (this study), together with observations from the FG/KSAT-1358 database compiled by Feng and Vardanega [26,27]. Note that only the selected range of  $k$  is shown. Based on the notable overlap of the datasets in Figure 12a, the data from the FI-CLAY-oedo/14/282 database is in accordance with FG/KSAT-1358. However, as illustrated in Figure 12b, even though FI-CLAY-oedo/14/282 data is, for the most part, in accordance with the transformation models derived by Feng and Vardanega [26], there is no notable correlation. The authors estimate that since FI-CLAY-oedo/14/282 consists mostly of soft marine clay soils, the range in  $k_L$  value is too narrow to show a significant correlation with  $w_n/w_L$ . Therefore, no transformation model for hydraulic conductivity was derived in this study.

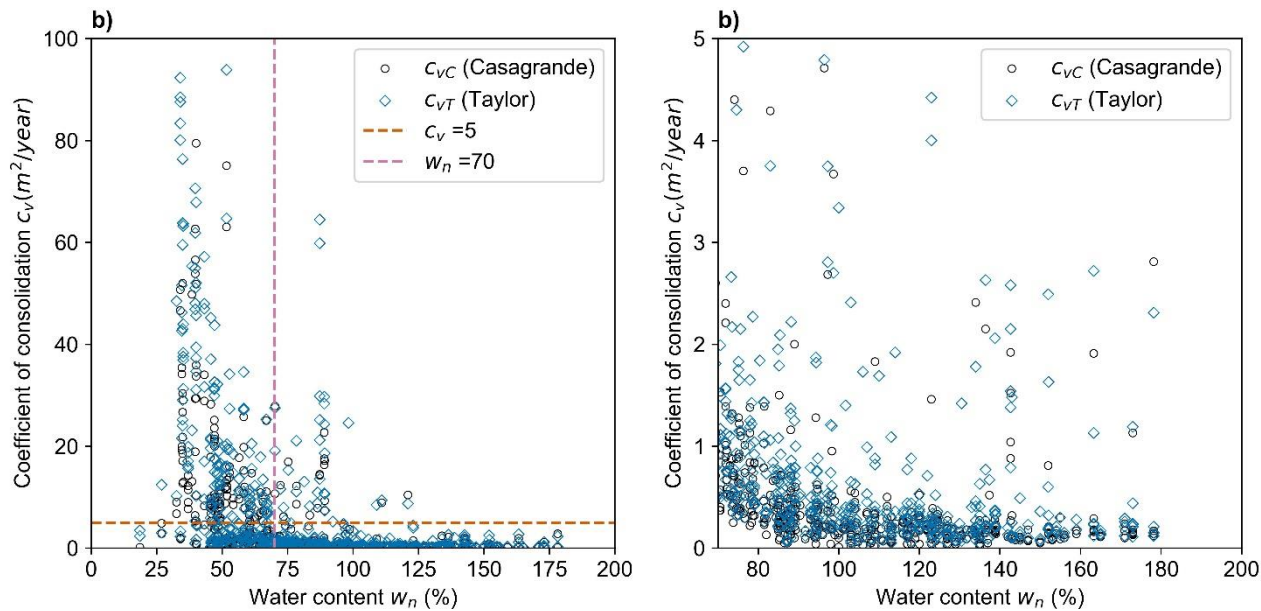


**Figure 11.** Relationship between  $w_n$  and  $c_v$ . (a) All observations (FI-CLAY-cv/8/774); (b)  $w_n > 70\%$  and  $c_v \leq 5 \text{ m}^2/\text{year}$ .

### 3.3.2. Creep coefficient

Figure 13a shows the relationship between the creep coefficient [ $C_{ae}$  in NC state (stress ratio  $> 0.8$ ) and  $C_{ae,max}$ ] and  $w_n$ . Maximum creep  $C_{ae,max}$  seems to form the upper bound, as expected. The figure also shows the area in which observations on Swedish soft soils are located [15]; data from FI-CLAY-oedo/14/282 shows a similar positive correlation between  $w_n$  and  $C_{ae,max}$ . Meanwhile, Figure 13b shows the dependence between  $w_n$  and  $C_{ae}$  in the OC state (stress ratio  $\leq 0.8$ ); some positive correlation can be observed, but the strength of the correlation and the amount of data were assessed to be too small to derive reliable transformation model for  $C_{ae}$  in the OC state.

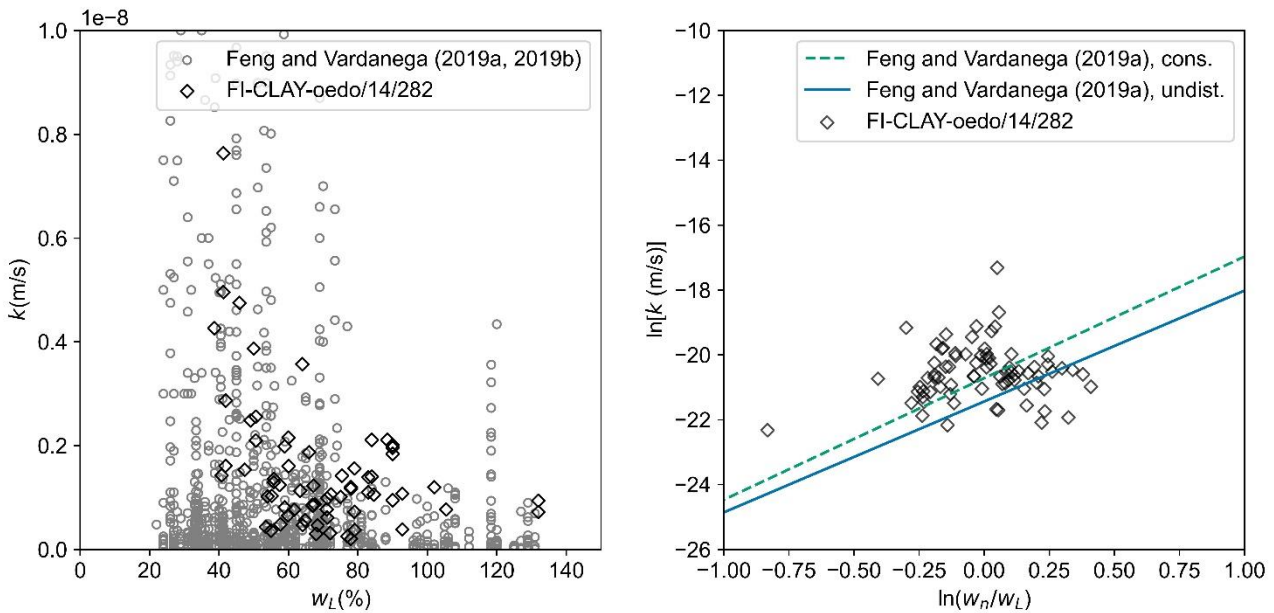


**Figure 12.** Validation of the FI-CLAY-oedo/14/282 database against the FG/KSAT-1358 database [26,27]. (a) Relationship between  $w_L$  and  $k$ ; (b) prediction of  $k$  based on  $w_n/w_L$  (cons. = consolidated disturbed specimen; undist. = undisturbed specimen).

Figure 14 illustrates the relationship between compressibility and creep coefficient  $C_{ae,max}$ . Figure 14b compares the data with Andersen's [28] transformation model for  $C_{ae}$ , which uses compression ratio CR [=  $C_C/(1+e_0)$  given in %] as a predictor: this Danish model for clays, gyttjas, and peats is found to somewhat overestimate  $C_{ae,max}$  for Finnish clay and gyttja soils. When the Andersen's best fit model ( $C_{ae} = 0.009\text{CR}^{1.58}$ ) was used to predict  $C_{ae,max}$  in FI-CLAY-oedo/14/282, the average model bias (Equation 5) was found to be 0.74 with transformation uncertainty  $\delta = 0.57$ .

Linear or polynomial transformation models for  $C_{ae,max}$  were derived using three predictors:  $C_C$ ,  $w_n$ , and  $e_0$ . The model statistics and regression coefficients are collected in Table 5. Figures 15a and 16a illustrate the fitted transformation model with ln-transformed variables ( $w_n$  or  $C_C$ ) as axes, while Figures 15b and 16a show the predicted vs. actual  $C_{ae,max}$  scatterplot with 1:1 line and  $\pm 50\%$  boundaries. The mean bias values for the  $C_{ae,max}$  models are around 1.1, but the medians for the bias are approximately 1.0, which implies that the distributions of the biases are skewed (e.g., lognormal rather than normal distribution). A median or mean equal to 1 should be expected, as the transformation model is derived using the same dataset to which its prediction is compared; in other words, the studied model should be unbiased. One outlier was detected using the  $3\sigma$ -threshold when fitting the  $C_{ae,max}(C_C)$  model. For these transformation models, the transformation uncertainty is  $\delta = 0.43\text{--}0.47$ , which implies medium transformation uncertainty [29].

Next, the relationship between  $c_v$  and  $C_{ae}$  was investigated. Such transformation model would be useful if the load increment has not been long enough to provide a reliable  $C_{ae}$  estimate; the  $c_v$  for that load increment, defined with either Taylor or Casagrande methods, could then be used to estimate  $C_{ae}$ . Such a model may also be applied to the CRS test, as it provides a  $c_v$  value. Figure 17 presents the derived linear  $C_{ae}(c_{vT})$  model and the detected outlier values. Table 5 presents the statistics for both  $C_{ae}(c_{vT})$  and  $C_{ae}(c_{vC})$  models; the transformation uncertainty is found to be smaller when  $c_{vC}$  is the predictor ( $\delta = 0.56$  versus  $\delta = 0.64$ ).

**Table 5.** Statistics for derived transformation models for the coefficient of creep.

Model variables		Outliers	Regression model: $Y = b_0 + b_1X + b_2(X)^2 + \varepsilon$					Bias statistics			
$Y$	$X$		$b_0$	$b_1$	$b_2$	$\sigma_\varepsilon$	$n$	$R^2$	50%	Mean	$\delta$
	$\ln(C_C)$	1	0.2784	0.843	(0)	0.435	154	0.69	1.00	1.10	0.43
$\ln(C_{\alpha\epsilon, \max})$	$\ln(w_n)$	0	-13.157	4.746	-0.377	0.469	166	0.64	1.01	1.11	0.47
	$\ln(e_o)$	0	-0.9751	2.109	-0.423	0.468	166	0.64	1.00	1.11	0.46
$\ln(C_{\alpha\epsilon})$	$\ln(c_{vT})$	4	-0.330	-0.445	(0)	0.596	694	0.66	0.99	1.19	0.64
	$\ln(c_{vC})$	5	-0.522	-0.480	(0)	0.548	674	0.71	1.00	1.16	0.56

Notes:  $n$  = number of observations used to fit the model;  $R^2$  = degree of determination;  $\sigma_\varepsilon$  = standard deviation of the zero-mean transformation error  $\varepsilon$ ; 50% = median;  $\delta$  = COV of the bias values.

Finally, Figure 18a shows the  $C_{\alpha\epsilon, \max}(w_n)$  model in linear scale together with  $\pm 2\sigma_\varepsilon$  boundaries, showing that in small  $w_n$  values, the model is characterized by smaller transformation uncertainty, which is in accordance with the observations [same for  $C_{\alpha\epsilon, \max}(C_C)$  model, see Figure 14a]. Accordingly, Figure 18b shows the derived  $C_{\alpha\epsilon}(c_{vT})$  model in linear scale. Due to the strong nonlinearity of the model, it is evident that the transformation model should not be applied blindly to very small  $c_v$  values. If the transformation model predicts  $C_{\alpha\epsilon} > 6$ , it is recommended to use an estimated maximum value instead.

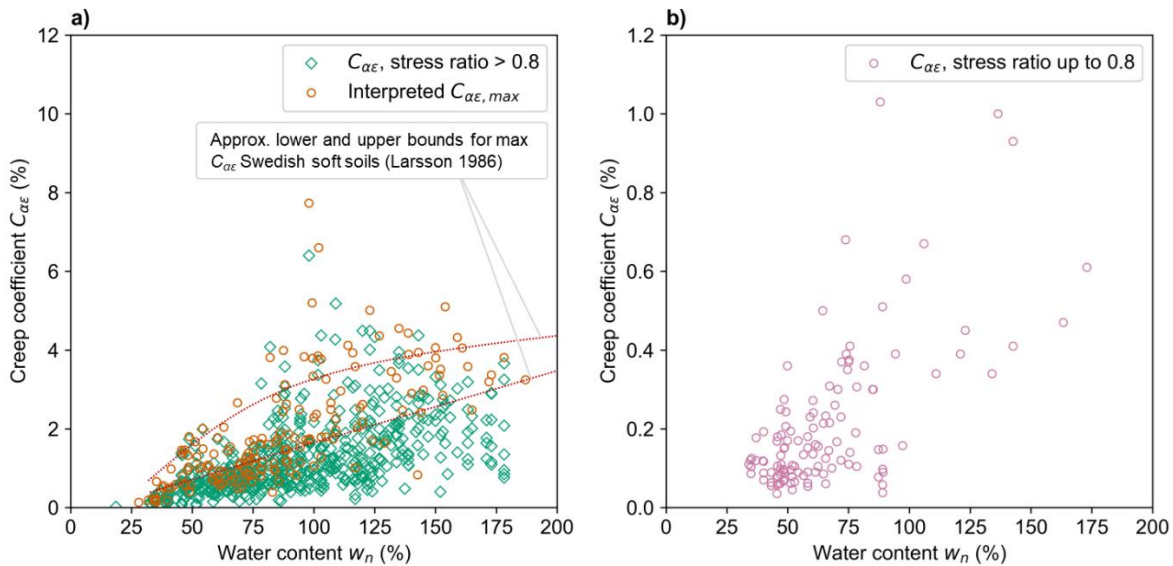


**Figure 13.** Relationship between  $w_n$  and (a)  $C_{\alpha\epsilon}$  in NC state (stress ratio > 0.8) and  $C_{\alpha\epsilon, \max}$  (this study), compared with max  $C_{\alpha\epsilon}$  reported by Larsson [15]; and (b)  $C_{\alpha\epsilon}$  in OC state (stress ratio  $\leq 0.8$ ).

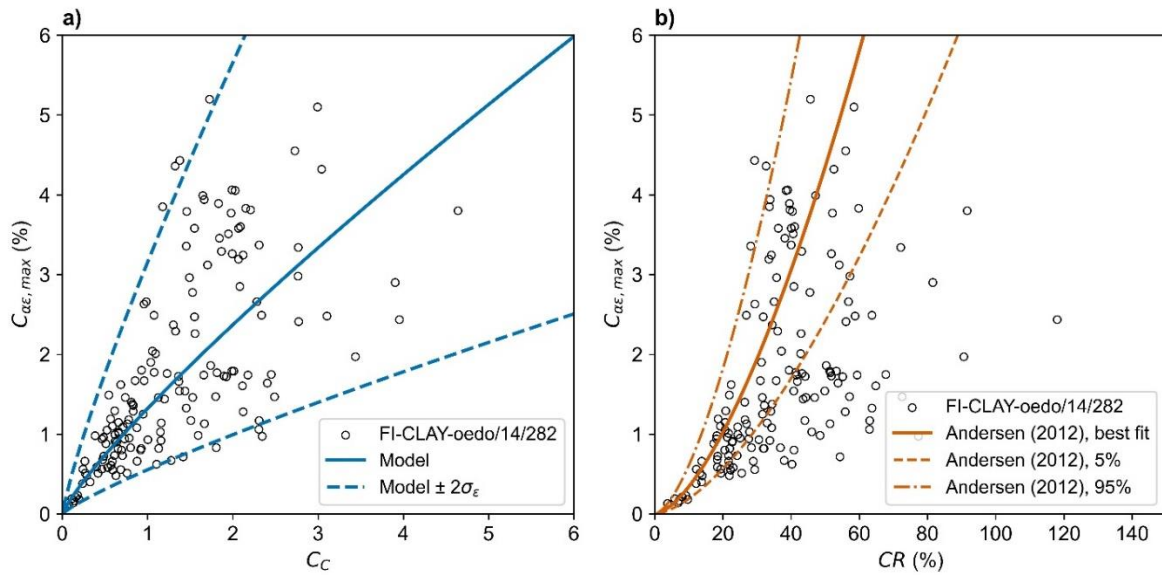


**Figure 14.** Relationship between compressibility and creep. (a) compression index  $C_c$  vs.  $C_{ae,max}$  (data and fitted model); (b) compression ratio CR vs.  $C_{ae,max}$  data together with Andersen's [28] model for  $C_{ae}$ .

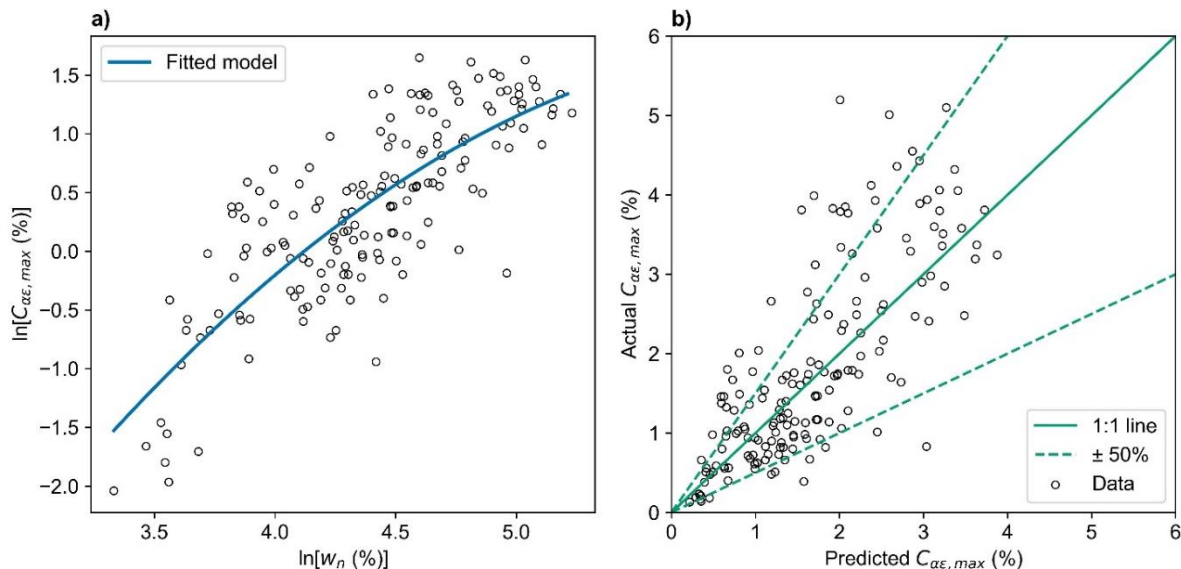


**Figure 15.** Prediction of  $C_{ae,max}$  based on  $w_n$ : (a) fitted polynomial regression model and (b) predicted vs. actual values.

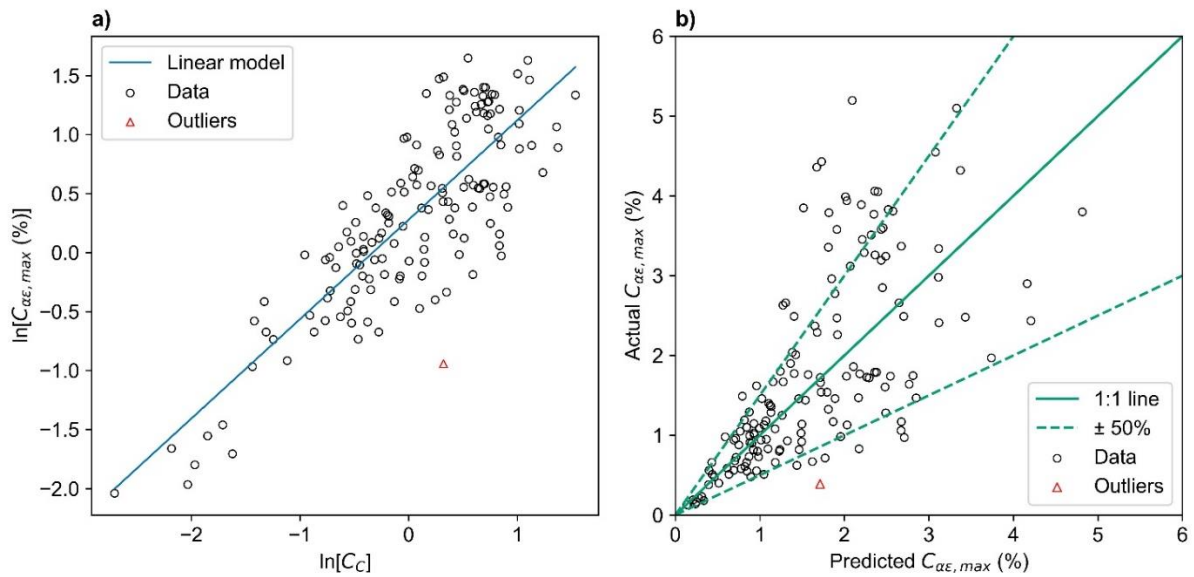


**Figure 16.** Prediction of  $C_{\alpha\epsilon, \max}$  based on  $C_C$ : (a) fitted linear regression model and (b) predicted vs. actual values.

To compare, the transformation uncertainty in the models to predict creep coefficient ( $\delta \approx 0.4$ –0.6) is found to be somewhat larger than the transformation models for compressibility (e.g.,  $C_C$ ) of Finnish clay soils,  $\delta \approx 0.4$  [6]. (To compare, the TC304 state-of-the-art report [30] observed that most clay models for  $C_C$  and  $C_S$  have high variability, i.e.,  $0.6 < \delta < 0.9$ .)

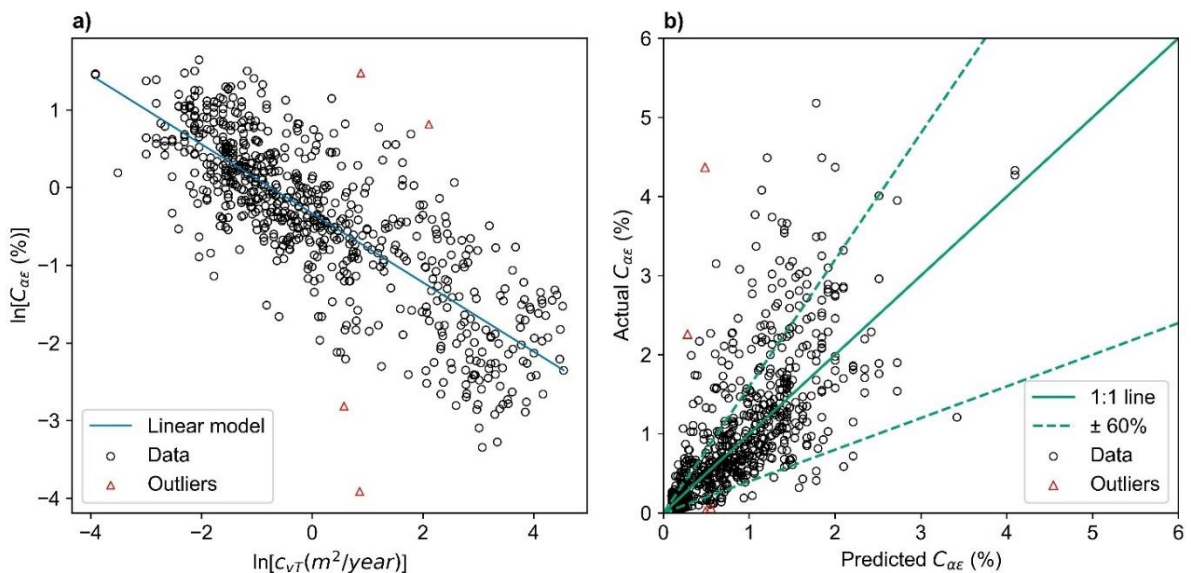


**Figure 17.** Prediction of  $C_{\alpha\epsilon}$  based on  $c_{vT}$  of the same stress increment: (a) fitted linear regression model and (b) predicted vs. actual values.

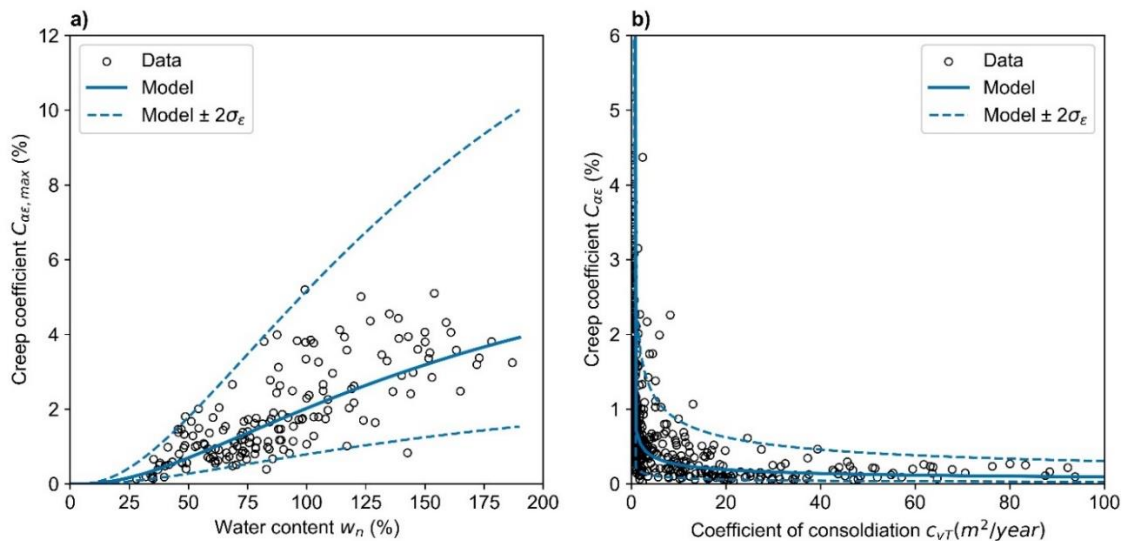


**Figure 18.** Transformation models to predict consolidation properties: (a)  $C_{ae,max}$  based on  $w_n$ ; (b)  $C_{ae}$  based on  $c_{vT}$  of the same stress increment.

### 3.4. Typical value distributions for consolidation properties

The typical value distributions of  $c_v$  were formed for two data groups: (1) soil specimens with  $w_n > 70\%$ , categorized as soft soils (i.e., clay and gyttja soils), and (2) soil specimens with  $w_n \leq 70\%$ , categorized as stiff clays and silts. In addition,  $c_v$  values corresponding to OC or NC states were separated. However, instead of using stress ratio  $\sigma_v'/\sigma_p' = 1$  as the defining boundary, to account for possible measurement error in  $\sigma_p'$ , the following definitions were used:  $\sigma_v'/\sigma_p' < 0.9$  was categorized as OC state, while  $\sigma_v'/\sigma_p' > 1.1$  was categorized as NC state. In the case of creep coefficient  $C_{ae}$ , load increment specific values were separated to OC and NC states using the critical stress  $0.8\sigma_p'$  (that is, stress ratio  $\sigma_v'/\sigma_p' = 0.8$ ). As above, to account for possible measurement errors, the datasets were formed using the criteria  $\sigma_v'/\sigma_p' < 0.7$  and  $\sigma_v'/\sigma_p' > 0.9$ .

In the determination of a typical value distribution of hydraulic conductivity  $k$ , an effort was made to evaluate the initial (natural state)  $k$ . The parameter  $k_I$  provides this estimate, but another dataset was formed by considering load increment specific  $k$  values: stress ratios  $\sigma_v'/\sigma_p' < 2$  were estimated to provide approximations of  $k_I$ . Estimates based on Taylor and Casagrande methods ( $k_T$  and  $k_C$ ) were considered as separate datasets. After stress ratio filtering, the number of  $k_{direct}$  values ( $n = 49$ ) was assessed to be too small to form a typical value distribution. Further division of data into soft soils and stiffer soil specimens was trialed, but the change in the typical value distribution was considered to be insignificantly small; these results were hence omitted.

The typical value distributions for  $c_v$  are shown in Figure 19 (soft soils) and Figure 20 (stiff clays and silts), and their statistics and parameters for lognormal distribution (MLE fit) are collected in Table 6. The minimum  $c_v$  from the CRS test ( $c_{v,min}$ ) was found to have a very similar distribution to the  $c_v$  in NC state, and hence these datasets were combined to form a typical value distribution (Figure 19a). Nonetheless, the statistics are provided for distinct datasets also in Table 6. For soft soils, there is a clear distinction between the typical values in NC state compared to OC state; the mean value for  $c_v$  in OC state is, on average, approximately 10 times greater. It is also observed that the mean value for  $c_v$  in NC

state is rather small, on the scale of  $0.5 \text{ m}^2/\text{year}$ . In stiff clays and silts, however, the difference between OC and NC states is much smaller. The mean  $c_v$  value in NC state for stiff clays and silts ( $7 \text{ m}^2/\text{year}$  and  $13 \text{ m}^2/\text{year}$ ) is in accordance with the typical values (for  $c_v$  slightly above  $\sigma_p'$ ) suggested for Danish inorganic clay ( $16 \text{ m}^2/\text{year}$ ) and gytta or organic clay ( $6 \text{ m}^2/\text{year}$ ) [28]. Very high COV values are observed for all  $c_v$  data groups, ranging from 0.9 to 2.1 (Table 6). Such high COV values can be expected because consolidation properties are known to have large inherent variability even within semi-homogeneous soil layers. For the inherent variability of  $c_v$ ,  $\text{COV}_{\text{inh}} = 0.33\text{--}0.68$  has been suggested [31], and  $\text{COV}_{\text{inh}} = 0.28\text{--}0.61$  has been observed to apply to soft Finnish clays [32].

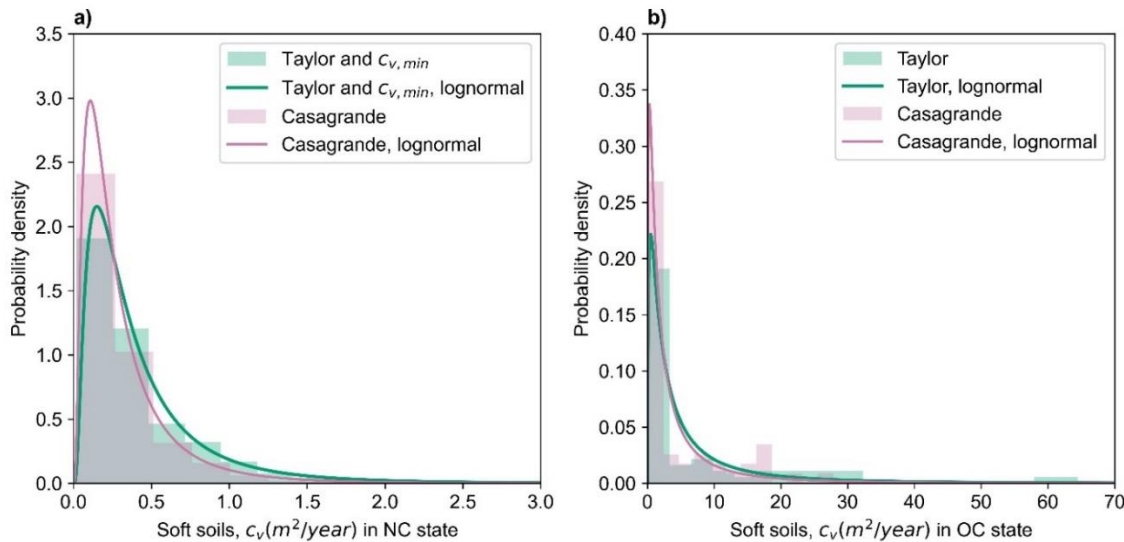


**Figure 19.** Typical value distributions of  $c_v$  for soft soils ( $w_n > 70\%$ ) in (a) NC state and (b) OC state (FI-CLAY-cv/8/774).

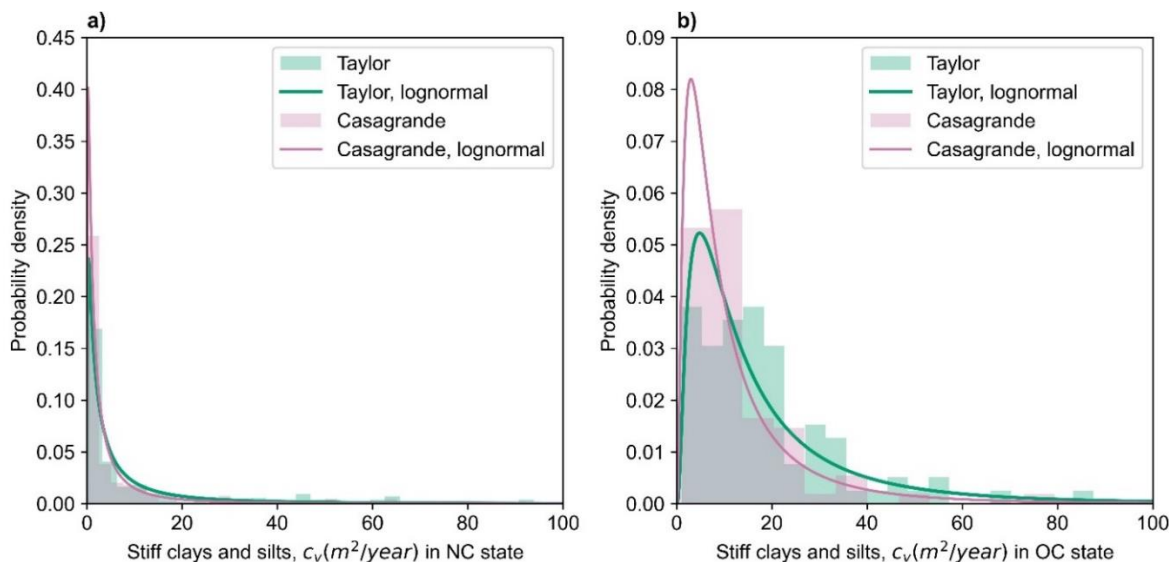


**Figure 20.** Typical value distributions of  $c_v$  for stiff clays and silts ( $w_n \leq 70\%$ ) in (a) NC state and (b) OC state (FI-CLAY-cv/8/774).

**Table 6.** Statistics for the typical values and MLE distribution fit.

Dataset	Statistics (arithmetic)							Lognormal distribution	
	<i>n</i>	min	50%	max	mean	SD	COV	$\mu_{ln}$	$\sigma_{ln}$
Soft soils (clays and gyttja soils), $w_n = 70\text{--}190\%$ :									
$c_{vT}$ in NC state (inlc. $c_{vmin}$ )	484	0.02	0.29	11.6	0.488	0.838	1.716	-1.165	0.8566
$c_{vT}$ in NC state	402	0.02	0.30	11.60	0.504	0.857	1.701	-1.141	0.8772
$c_{vmin}$ (in NC state)	82	0.05	0.25	6.50	0.412	0.736	1.736	-1.284	0.7361
$c_{vC}$ in NC state	384	0.02	0.22	12.34	0.358	0.750	2.092	-1.491	0.8620
$c_{vT}$ in OC state	57	0.15	2.15	64.46	8.897	13.57	1.525	1.226	1.3920
$c_{vC}$ in OC state	50	0.13	1.92	27.85	5.328	6.741	1.265	0.814	1.4032
Stiff clays and silts, $w_n = 20\text{--}70\%$ :									
$c_{vT}$ in NC state	174	0.09	2.67	93.85	12.55	20.59	1.641	1.322	1.5887
$c_{vC}$ in NC state	158	0.09	1.43	75.05	6.821	13.68	2.005	0.701	1.4863
$c_{vT}$ in OC state	91	1.00	15.6	87.56	18.44	15.59	0.845	2.533	0.9781
$c_{vC}$ in OC state	83	0.64	8.74	79.44	12.12	11.77	0.971	2.082	0.9933
Clay and gyttja soils, $w_n = 20\text{--}190\%$ :									
$C_{ae,max}$	168	0.13	1.48	7.73	1.902	1.358	0.714	0.369	0.7940
$C_{ae}$ in “NC” state	563	0.02	0.97	6.40	1.227	0.911	0.743	-0.070	0.7888
$C_{ae}$ in “OC” state	107	0.04	0.13	1.03	0.187	0.163	0.871	-1.931	0.6785
$k_l$ (oedometer)	282	0.07	0.86	30.2	1.373	2.226	1.620	-0.118	0.8573
$k_T$ (stress ratio < 2)	202	0.011	0.59	4.39	0.740	0.661	0.893	-0.690	0.9894
$k_C$ (stress ratio < 2)	185	0.017	0.39	2.773	0.491	0.445	0.906	-1.107	0.9842

Notes on units:  $c_v$  values are in  $\text{m}^2/\text{year}$ ,  $C_{ae}$  values are in %, and  $k$  values are in  $10^{-9} \text{ m/s}$ .

Typical value distributions for creep coefficients of clay and gyttja soils (i.e., all the data in the compiled databases) are shown in Figure 21, and their statistics are collected in Table 6. There is approximately a ten-times difference in the mean and maximum values for  $C_{ae}$  in OC state compared to  $C_{ae,max}$  and  $C_{ae}$  in NC state. The COV value for creep coefficients varies between 0.7 and 0.9. As expected, this is a somewhat larger COV value compared to the inherent variability of  $C_{ae}$  observed in Finnish clays,  $\text{COV}_{inh} = 0.26\text{--}0.52$  [32].

Finally, typical value distributions for hydraulic conductivity  $k$  are shown in Figure 22. As expected, the mean value for  $k_l$  is greater than for the data groups with  $k$  values (even though the stress ratio is limited to 2). As for COV,  $k_l$  has the greatest value (1.6), while  $k$  values have  $\text{COV} \approx 0.9$ . For the inherent variability of  $k$ ,  $\text{COV}_{inh} = 0.68\text{--}0.90$  has been suggested [31]. Meanwhile, for  $k_l$  of soft Finnish clays, a range equal to  $\text{COV}_{inh} = 0.29\text{--}0.56$  has been observed [32].

According to Figures 19–22, a lognormal distribution seems to fit the datasets rather well. Note that for better readability of the histograms, the x-axes for NC  $c_v$  of soft soils (Figure 19a) and  $k_l$

(Figure 22b) have been limited to a value smaller than the maximum observed value, since those high value occurrences were too rare to be seen in the histogram.

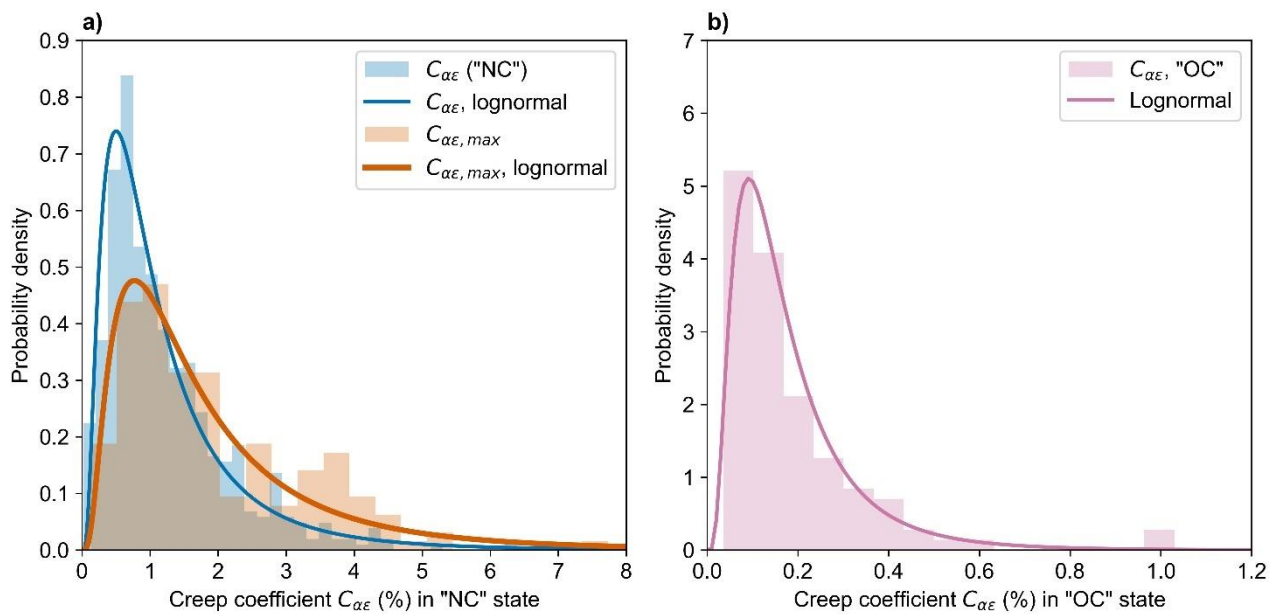


**Figure 21.** Typical value distributions of  $C_{\alpha\epsilon}$  for clay and gyttja soils: (a)  $C_{\alpha\epsilon,max}$  and  $C_{\alpha\epsilon}$  in NC state and (b)  $C_{\alpha\epsilon}$  in OC state (FI-CLAY-cv/8/774 and FI-CLAY-oedo/14/282).

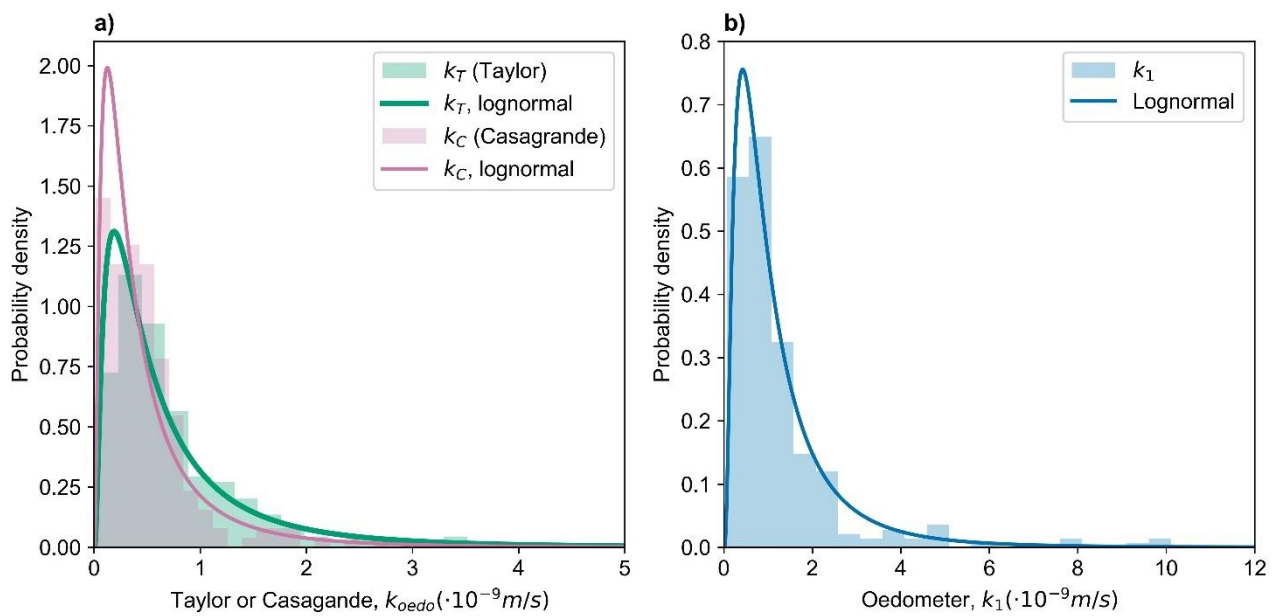


**Figure 22.** Typical value distributions of  $k$  for clay and gyttja soils: (a)  $k_T$  and  $k_C$  for stress ratios < 2 (FI-CLAY-cv/8/774); and (b) interpreted  $k_1$  (FI-CLAY-oedo/14/282).

#### 4. Conclusions

This paper introduced and investigated two compiled databases of consolidation properties for Finnish clay and gyttja soils: FI-CLAY-oedo/14/282 contains oedometer test-specific parameters such as initial hydraulic conductivity  $k_I$  and maximum creep coefficient  $C_{ae,max}$ , while FI-CLAY-cv/8/774 consists of load increment-specific parameters such as coefficient of consolidation  $c_v$  and hydraulic conductivity  $k$ . The analysis of these databases provided three main results:

- 1) Statistics for bias factors, which quantify the difference between methods to define  $c_v$  and  $k$  (e.g., Taylor vs. Casagrande methods, oedometer test vs. falling head test).
- 2) Linear or polynomial transformation models (and their transformation uncertainty) to predict the creep coefficient ( $C_{ae,max}$  or  $C_{ae}$ ) from index or consolidation properties.
- 3) Typical value distributions in the form of histograms and fitted lognormal distributions for various consolidation properties ( $c_v$ ,  $k$ ,  $C_{ae,max}$ , and  $C_{ae}$ ).

All the results are given with statistical information, which allows their straightforward utilization as input data for probabilistic assessment (reliability-based design, RBD). After all, consolidation properties based on transformation models or typical value distributions are both characterized by significant uncertainty, and hence RBD enables assessing the corresponding uncertainty in the settlement prediction [33].

The statistics of the bias factors revealed that the  $c_v$  defined using the Casagrande (log time) method is, on average, 0.8 times the  $c_v$  defined with the Taylor (square root time) method. A comparison between the falling head test (i.e., direct measurement) and incremental oedometer test showed that  $k_{direct}$  was, on average, 1.4 times the  $k$  value, according to Taylor. The Casagrande method was found to have an even greater bias (1.8). Meanwhile, the transformation uncertainty in the models to predict creep coefficient was found to be  $\delta \approx 0.4\text{--}0.6$  ( $\delta$  is the coefficient of variation COV for a transformation model). For example, the transformation uncertainty in the regression model to predict  $C_{ae,max}$  from  $w_n$  was  $\delta = 0.47$  (i.e., 47%). The smallest transformation uncertainty ( $\delta = 0.43$ ) was acquired when the compression index  $C_C$  was used as a predictor for  $C_{ae,max}$ . Since the dataset contained Finnish clay and gyttja soils only, the derived transformation models may be biased if applied outside of Finland. However, the authors estimate that the derived transformation models can be applied with relatively small bias to clay and gyttja deposits on the eastern coast of Sweden due to shared geological sedimentation history (i.e., post-glacial clays deposited in the Baltic Sea).

It was observed that the typical value distributions of consolidation properties of Finnish soft soils, stiff clays, or silts are characterized by COV in the scale of 1.0–2.0 (i.e., 100–200%). In soft soils ( $w_n = 70\text{--}190\%$ ), the mean value for  $c_v$  in the over-consolidated state was found to be, on average, around ten times greater than  $c_v$  in the normally consolidated state. To conclude, the consolidation properties of clay and gyttja soils are marked with considerable uncertainty. Hence, it is beneficial to consider the existing knowledge when determining the soil parameters either by supporting engineering judgement or via a more systematic framework such as Bayesian statistics [34].

In the future, possibly reducing the considered transformation uncertainties by means of advanced machine learning algorithms should be investigated. Support vector machine, random forest, and artificial neural networks could be used to create transformation models for the consolidation rate and creep properties of clay and gyttja soils with reduced transformation uncertainty [35,36]. Moreover, with the novel machine learning algorithms' capacity to analyze big

data (e.g., [35]), the compiled databases could be further extended, and the transformation models refitted with the complemented datasets.

### Use of AI tools declaration

The authors declare they have not used Artificial Intelligence (AI) tools in the creation of this article.

### Author contributions

M S Löfman: Methodology, Software, Validation, Formal analysis, Writing—Original Draft, Visualization. L Korkiala-Tanttu: Conceptualization, Supervision, Resources, Writing—Review & Editing.

### Acknowledgments

The authors would like to acknowledge Finnish Transport Infrastructure Agency for funding the compilation of these databases. Special gratitude is forwarded to Matti Lojander who supervised the test procedure and parameter interpretation for most of the oedometer tests included in the databases.

### Conflict of interest

All authors declare no conflicts of interest in this paper.

### References

1. Perttu O, Vicente S, Löfman M, et al. (2024) Carbon management in geotechnical engineering solutions, *Geotechnical Engineering Challenges to Meet Current and Emerging Needs of Society*, CRC Press, 3228–3232.
2. Kivi E (2022) Pohjanvahvistusmenetelmät Suomessa—Käytönmäärät ja hiilijalanjälki. Espoo: Aalto University. Available from: <https://aaltodoc.aalto.fi/items/0a309556-72a4-468b-b089-cd6da2ec962a>.
3. Lee IK, White W, Ingles OG (1983) *Geotechnical Engineering*, Boston: Pitman.
4. Leroueil S, Magnan J-P, Tavenas F (1990) *Embankments on Soft Clay*, Chichester: Ellis Horwood.
5. Gardemeister R (1975) On engineering-geological properties of fine-grained sediments in Finland. 91.
6. Löfman MS, Korkiala-Tanttu LK (2022) Transformation models for the compressibility properties of Finnish clays using a multivariate database. *Georisk Assess Manage Risk Eng Syst Geohazards* 16: 330–346. <https://doi.org/10.1080/17499518.2020.1864410>
7. D'Ignazio M, Phoon KK, Tan SA, et al. (2016) Correlations for undrained shear strength of Finnish soft clays. *Can Geotech J* 53: 1628–1645. <https://doi.org/10.1139/cgj-2016-0037>

8. Baecher GB (2019) Putting Numbers on Geotechnical Judgment. Companion whitepaper to the 27th Buchanan Lecture, Texas A&M University. Available from: [https://www.researchgate.net/publication/338801782\\_Baecher\\_2019\\_-Putting\\_Numbers\\_on\\_Geotechnical\\_Judgment\\_27th\\_Buchanan\\_Lecture](https://www.researchgate.net/publication/338801782_Baecher_2019_-Putting_Numbers_on_Geotechnical_Judgment_27th_Buchanan_Lecture).
9. Cao Z, Wang Y, Li D (2016) Quantification of prior knowledge in geotechnical site characterization. *Eng Geol* 203: 107–116. <https://doi.org/10.1016/j.enggeo.2015.08.018>
10. Wang Y, Cao Z, Li D (2016) Bayesian perspective on geotechnical variability and site characterization. *Eng Geol* 203: 117–125. <https://doi.org/10.1016/j.enggeo.2015.08.017>
11. Taylor DW (1948) *Fundamentals of Soil Mechanics*, New York, John Wiley & Sons Inc.
12. Casagrande A (1936) The determination of preconsolidation load and its practical significance. *Proc 1st Int Conf Soil Mech*.
13. Buisman A (1936) Results of Long Duration Settlement Tests. *Int Conf Soil Mech Found Eng*, 103–106.
14. Mesri G, Choi YK (1985) The uniqueness of the end-of-primary (EOP) void ratio-effective stress relationship. 587–590.
15. Larsson R (1986) *Consolidation of soft soils*, Linköping.
16. Mesri G, Castro A (1987) C a/C c concept and K 0 during secondary compression. *J Geotech Eng* 113: 230–247. [https://doi.org/10.1061/\(ASCE\)0733-9410\(1987\)113:3\(230\)](https://doi.org/10.1061/(ASCE)0733-9410(1987)113:3(230))
17. Mataić I (2016) On structure and rate dependence of Perniö clay.
18. Suhonen K (2010) Creep of Soft Clay. Master thesis, Aalto University. 103. Available from: <https://aaltodoc.aalto.fi/server/api/core/bitstreams/05a2a28b-aadd-4878-aa25-62a179ee52be/content>.
19. Korhonen KH, Gardemeister R, Tammirinne M (1974) Geotekninen maaluokitus. Geotekniikan laboratorio, tiedonanto 14. Otaniemi, Espoo. Available from: [https://publications.vtt.fi/julkaisut/muut/1970s/geotekniikan\\_tiedonanto\\_14.pdf](https://publications.vtt.fi/julkaisut/muut/1970s/geotekniikan_tiedonanto_14.pdf).
20. Koskinen M (2014) Plastic Anisotropy and Destructuration of Soft Finnish Clays. Espoo: Aalto University.
21. Phoon K-K, Kulhawy FH (1999) Characterization of geotechnical variability. *Can Geotech J* 36: 612–624. <https://doi.org/10.1139/t99-038>
22. Ching J, Phoon K-K (2014) Transformations and correlations among some clay parameters—The global database. *Can Geotech J* 51: 663–685. <https://doi.org/10.1139/cgj-2013-0262>
23. Pedregosa F, Varoquaux G, Gramfort A, et al. (2011) Scikit-learn: Machine Learning in Python. *J Mach Learn Res* 12: 2825–2830.
24. Ang AHS, Tang WH (2006) Probability Concepts in Engineering: Emphasis on Applications to Civil and Environmental Engineering. *Wiley*, 432.
25. Berilgen SA, Berilgen MM, Ozaydin IK (2006) Compression and permeability relationships in high water content clays. *Appl Clay Sci* 31: 249–261. <https://doi.org/10.1016/j.clay.2005.08.002>
26. Feng S, Vardanega PJ (2019) Correlation of the hydraulic conductivity of fine-grained soils with water content ratio using a database. *Environ Geotech* 6: 253–268. <https://doi.org/10.1680/jenge.18.00166>
27. Feng S, Vardanega PJ (2019) A database of saturated hydraulic conductivity of fine-grained soils: probability density functions. *Georisk Assess Manage Risk Eng Syst Geohazards* 13: 255–261. <https://doi.org/10.1080/17499518.2019.1652919>

28. Andersen JD (2012) Prediction of compression ratio for clays and organic soils. Proceedings of the 16th Nordic Geotechnical Meeting, Copenhagen, 1: 303–310.
29. Phoon K-K, Tang C (2019) Characterisation of geotechnical model uncertainty. *Georisk Assess Manage Risk Eng Syst Geohazards* 13: 101–130. <https://doi.org/10.1080/17499518.2019.1585545>
30. Ching J, Noorzad A (2021) Statistics for transformation uncertainties. State-of-the-art review of inherent variability and uncertainty in geotechnical properties and models, 171–180.
31. Uzielli M, Lacasse S, Nadim F, et al. (2006) Soil variability analysis for geotechnical practice. *Charact Eng Prop Natural Soils* 3: 1653–1752.
32. Löfman MS, Korkiala-Tanttu LK (2021) Inherent variability of geotechnical properties for Finnish clay soils. 18th International Probabilistic Workshop. IPW 2021. Lecture Notes in Civil Engineering, Springer, Cham. [https://doi.org/10.1007/978-3-030-73616-3\\_32](https://doi.org/10.1007/978-3-030-73616-3_32)
33. Phoon K-K (2017) Role of reliability calculations in geotechnical design. *Georisk Assess Manage Risk Eng Syst Geohazards* 11: 4–21. <https://doi.org/10.1080/17499518.2016.1265653>
34. Ching J, Phoon K-K, Wu C-T (2022) Data-centric quasi-site-specific prediction for compressibility of clays. *Can Geotech J* 59: 2033–2049. <https://doi.org/10.1139/cgj-2021-0658>
35. Phoon K-K, Zhang W (2023) Future of machine learning in geotechnics. *Georisk Assess Manage Risk Eng Syst Geohazards* 17: 7–22. <https://doi.org/10.1080/17499518.2022.2087884>
36. Zhang W, Li H, Li Y, et al. (2021) Application of deep learning algorithms in geotechnical engineering: a short critical review. *Artif Intell Rev* 54: 5633–5673. <https://doi.org/10.1007/s10462-021-09967-1>

## Supplementary

The compiled databases FI-CLAY-cv/8/774 and FI-CLAY-oedo/14/282 are provided as supplementary files in Excel file format (.xlsx).



AIMS Press

© 2025 the Author(s), licensee AIMS Press. This is an open access article distributed under the terms of the Creative Commons Attribution License (<https://creativecommons.org/licenses/by/4.0>)